

MASTER'S DEGREE FINAL THESIS
Master's Degree in Interdisciplinary and Innovative Engineering

EFFECT OF CUTTING TOOL ASSISTED WITH VIBRATIONS ON TURNING MACHINED C45 SAMPLES



Author: Magnin Christophe
Director: Ramón Jerez Mesa
Co-Director: Jose Antonio Travieso Rodríguez
Call: June 2022

GLOSARY

C45: Referent to the AISI52100 alloy steel selected for ball burnishing balls.

DOE: Design Of Experiments.

NVAM: Non-Vibration Assisted Machining

VAM: Vibration Assisted Machining

Ra: The arithmetical mean deviation of the roughness profile

Vc: Cutting velocity

n: Spindle speed

FFT: the Fast Fourier Transform

ABSTRACT

This thesis aims to analyse the effect of a cutting tool assisted with 40-kHz vibration on C45 steel samples. It exposes the improvement of surface finish through vibration application and the different effects thus generated while machining process. The vibratory movement of the cutting tool is one-dimensional, and cutting tests are performed on a lathe machine.

The study is mainly divided into two stages: the analyses of the effect of vibration assistance, feed and tool angle on the cutting force and roughness by means of a design of experiment. Then, the observation and characterisation of the chips removal mechanism with a high-speed camera to characterize the influence of the vibratory effect on its formation. The state of art section provide knowledge to understand the subject by exposing all the research and studies similar from our topic to justify the experiments that will be carried out. All procedures to achieve the research objectives are described, including the experimental design, experimental setup and the materials used to conduct them.

It is concluded that one dimensional vibration assisted machining (VAM) offers distinct advantages over conventional machining (NVAM). The surface quality is improved when the cutting parameters are carefully implemented; adding vibration is the most significant effect on the surface quality providing lower Ra values than NVAM. VAM has demonstrated that applying vibration as a significative influence on the chip removal mechanism. Indeed, the chip fragmentation is facilitated by the VAM process by forming arc loose chips which ultimately improve the surface quality and tool wear resistance by limiting the friction due to enhanced evacuation of the chip. The texturization effects of VAM to obtain specific surface texture are also observed. From VAM to NVAM, two different patterns are easily detected (linear and mesh shape), the level intensity depends on the feed rate.

ACKNOWLEDGMENT

First, I would like to express my very great appreciation to my project director Ramón Jerez Mesa for his involvement in the project and all the constructive suggestions, encouragement, and useful critiques during the development of this research work.

Also thank to José Antonio Travieso and Jordi Llumà to help me and answering all my questions during the master project.

I would like to offer my special thanks to Youssef and Fadel, who assist me in carrying out the experiments.

I would also like to extend my thanks to the technicians of the laboratory for their help offering me knowledge to use the lathe.

Finally, I wish to thank my parents for their support and encouragement through my university studies in Spain.

Table of contents

GLOSARY	2
ABSTRACT	3
ACKNOWLEDGMENT	4
INDEX OF FIGURE	6
INDEX TABLES	7
1. Introduction	8
1.1 Preface	8
1.2 Objectives	8
2. State of the art	9
3. Materials and methods	13
3.1 Experimental design	13
3.1.1 Ishikawa chart	13
3.1.2 Experiment workflow	14
3.2 Experimental setup	15
3.2.1 Stage #1: Cutting tests (DOE)	15
3.2.2 Stage #2: Camera recording	19
3.3 Cutting tool characteristics	21
3.3.1 Cutting tool configuration	21
3.3.2 Prototype tool design	21
3.3.3 Insert type	22
3.4 Materials and specimens' geometry	23
3.5 Roughness acquisition system	24
3.5.1 Profilometer 2D	24
3.5.2 3D surface parameters and treatment	25
4. Results and analysis	27
4.1 Preliminary tests: determination of optimal V_c	27
4.2 Stage #1: Cutting tests	29
4.2.1. Influence of DOE factors on roughness results	29
4.2.2. Influence of DOE factors on cutting forces	33
4.2.3. Influence of DOE factors on chip formation	36
4.2.4. Influence of DOE factors on texture parameters S and V	40
4.3 Stage #2: Camera experiment	43
5. Conclusion	46
6. Bibliography	47
7. Annex	48

INDEX OF FIGURE

Figure 1 : Integration of multiple field and disciplines [1]	9
Figure 2 : Timeline of milestones in the development of UVAM [1].....	10
Figure 3 : Surface profile (um) depending on the machining process (VAM/conventional turning) [8]	12
Figure 4: Ishikawa chart description	13
Figure 5 : Experiments workflow.....	14
Figure 6 : Setup used to carry out the DOE experiment	15
Figure 7: KISTLER 9129AA multicomponent dynamometer and part designed.....	16
Figure 8: Depth of cut adjustment.....	17
Figure 9: Cutting forces on a lathe	18
Figure 10: C45 sample with DOE references.....	18
Figure 11: Camera experiment system.....	19
Figure 12: PCO 1200 s high speed camera	20
Figure 13: Cutting tool configuration and material associates.....	21
Figure 14: Prototype cutting tool V2 in section view	22
Figure 15: YG-1 DCMT070204-UF-YG3030 turning insert with a chipbreaker (source cutwell [11] and [16]).....	23
Figure 16: 2D profilometer SJ-210	24
Figure 17: STIL Micromeasure 2 3D-profilometer.....	26
Figure 18: Arithmetical mean deviation of the roughness profile (Ra) depending on the cutting velocity	28
Figure 19: Arithmetical mean deviation of the roughness profile (Ra) depending on the attribute.....	29
Figure 20: Pareto chart of the standardized effects response Ra.....	30
Figure 21: Residual plots for Ra	31
Figure 22: Main effects plot for Ra and P values.....	31
Figure 23: Interval plot for tool angle and feed rate.....	32
Figure 24: Interaction plot for Ra.....	33
Figure 25: Cutting forces f_x ; f_y and f_z depending on the attribute	34
Figure 26: Cutting forces f_x ; f_y and f_z of attribute B2C3 with and without vibration	35
Figure 27: Cutting forces f_x ; f_y and f_z amplified with feed rate increasing	35
Figure 28: Cutting forces f_x ; f_y and f_z expressed with Fourier transform.....	35
Figure 29: The arithmetical mean deviation of the roughness profile (Ra) depending on the attribute.....	37
Figure 30: Chips image from the DOE regarding level combination (attribute) without vibration	38
Figure 31: Chips image from the DOE regarding level combination (attribute) with vibration	39
Figure 32: Chip formation without vibration	44
Figure 33: Chip formation with vibration assisted.....	45

INDEX TABLES

Table 1: Factors and their level used for the DOE 16

Table 2: Machining parameters used for the DOE..... 17

Table 3: Factors and levels depending on the references 17

Table 4: Parameters used in the PCO software 20

Table 5: Manufacturing parameters used for the camera experiments 20

Table 6: YG-1 DCMT070204-UF-YG3030 Turning insert relevant parameters 23

Table 7: Chemical composition and mechanical properties of C45 steel 23

Table 8: 2D roughness parameters description (source 12) 25

Table 9: 3D texture parameters description (source 12) 26

Table 10: Manufacturing parameters from the supplier..... 27

Table 11: Manufacturing parameters used for the camera experiments 27

Table 12: Results from the optimal Vc experiments 27

Table 13: Results from the DOE without vibration (A1)..... 29

Table 14: Results from the DOE with vibration (A2)..... 29

Table 15: Chips results from the DOE 36

Table 16: 3D roughness parameters 40

Table 17: Visual aspect and bearing aera curve 42

Table 18: image processing parameters 43

1. Introduction

1.1 Preface

In the machining industry, manufacturing quality matters to ensure that the final products are able to meet the company's quality criteria. It also guarantees that the processes used to design, test, and produce a part is done correctly. Manufacturing quality should be in concordance to specifications from the customer or standard. An important aspect related to quality is the surface finish state, which affects the ability of the part to resist fatigue, avoid crack nucleation and propagation, corrosion and increase/decrease the friction. In a context where surface quality specifications are more and more exigent, vibration-assisted machining (VAM) is one of the techniques that has been adopted to improve the surface roughness and mechanical properties on the final workpiece compared to conventional manufacturing (non-vibration assisted machining, NVAM). Indeed, research related to this technology is growing in view of its many advantages in different field.

For instance, VAM allows the user to generate Taylor-made surfaces, with a specific texture pattern, it facilitates the removal of chips in brittle or difficult-to-cut materials and has also been cited for increasing productivity by increasing tool life in certain machining operations. Depending on how it is deployed and in what kind of technique (drilling, milling, burnishing etc.), VAM can be presented as a family of techniques with a great future to come. In this project, the VAM process to be studied is one-dimensional and performed on a lathe machine.

1.2 Objectives

This study aims to design, implement, and analyse the effect of a cutting tool assisted with vibration on cylindrical parts of C45 steel (lathe manufacturing). This research study focuses on characterize how the vibration vibratory effect affects both the material surface integrity (specifically its topology) and how the process occurs regarding chip removal and cutting dynamics.

The secondary objectives could be described as follows:

- Adapt and achieve an adequate setup configuration on the conventional lathe that allows to perform the cutting operation needed and equip it with different sensors to monitor how the process occurs.
- Observe and characterise the chips removal mechanism with a high-speed camera to characterize the influence of the vibratory effect on its formation.
- Observe and characterise the effect of vibration assistance, feed and tool angle on the cutting force demanded during the cutting operation and the roughness.
- Analyse the texturing effect of VAM on the surface roughness and 3D texture parameters compared to conventional manufacturing.

2. State of the art

The purpose of this section is to expose all the research and studies similar from our topic and related with the experiments that we will carry out. The aim is to provide knowledge to understand the improvement of surface finish through vibration application and the different effects thus generated during the machining process.

In the recent industry, machining by conventional turning offers a wide range of possible operations on all types of materials but is still very limited to machine advanced materials (such as brittle alloys or ceramics) used for specific applications such as optics etc. As exposed in the following section, adding vibration-assisted machining seems to improve surface finishing and mechanical properties on the final workpiece, even in those hard-to-machine materials. Surface quality is mainly affected by machining parameters, cutting tool properties, workpiece properties and cutting phenomena including vibrations. Research and improvements related to this technology are growing in view of its many advantages in terms of manufacturing finishing operation.

First, let's define VAM from a global point of view to understand and observe the basics of this technology. As shown in the figure 1, VAM integrates many fields and disciplines, as it can be executed in 1, 2 and 3 dimensions and in many and different machine-tools. In our case, the VAM process to be studied follows a radial one-dimensional vibration applied on orthogonal cutting with a lathe machine. One dimensional VAM system is the most common type due to its simple structure and ease of implementation. Generally, VAM is a non-traditional processing method that uses a transducer for converting high-frequency electrical energy into high-frequency mechanical vibrations energy and applies it to the machining process to realise material removal or deformation [1]. It includes a wide range of processes such as drilling, milling, grinding (traditional machining) as well as laser machining, electro-discharge machining, electro-chemical machining and burnishing (non-traditional machining) [2].

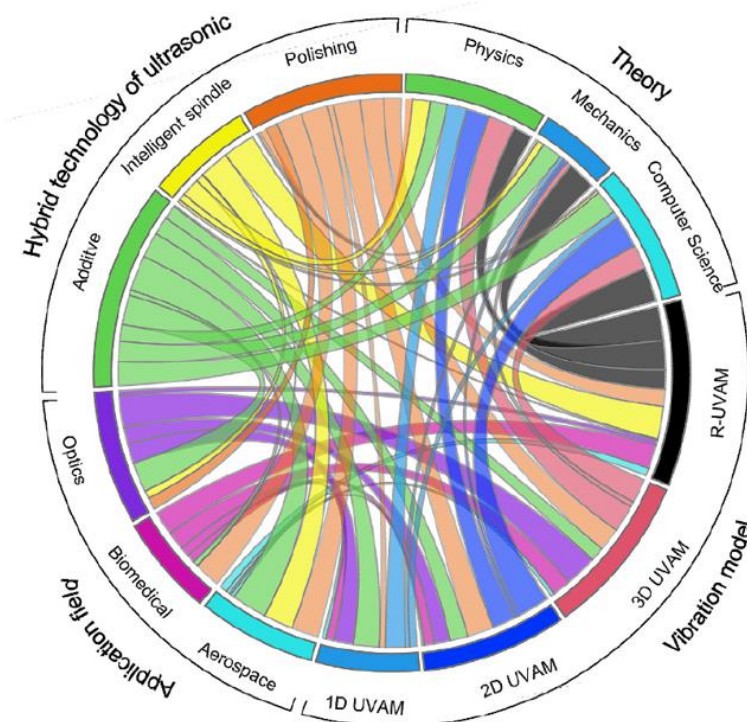


Figure 1 : Integration of multiple field and disciplines [1]

As shown in the figure 2, VAM was first introduced in the 60s, where the first rotary ultrasonic machining (RUM) model was developed. Then, the technologies resulting from the VAM process were developed over time. Around the 2000s, the development of VAM equipment became more complex introducing 2D and 3D VAM technologies which cover more application field such as biomedical and aerospace.

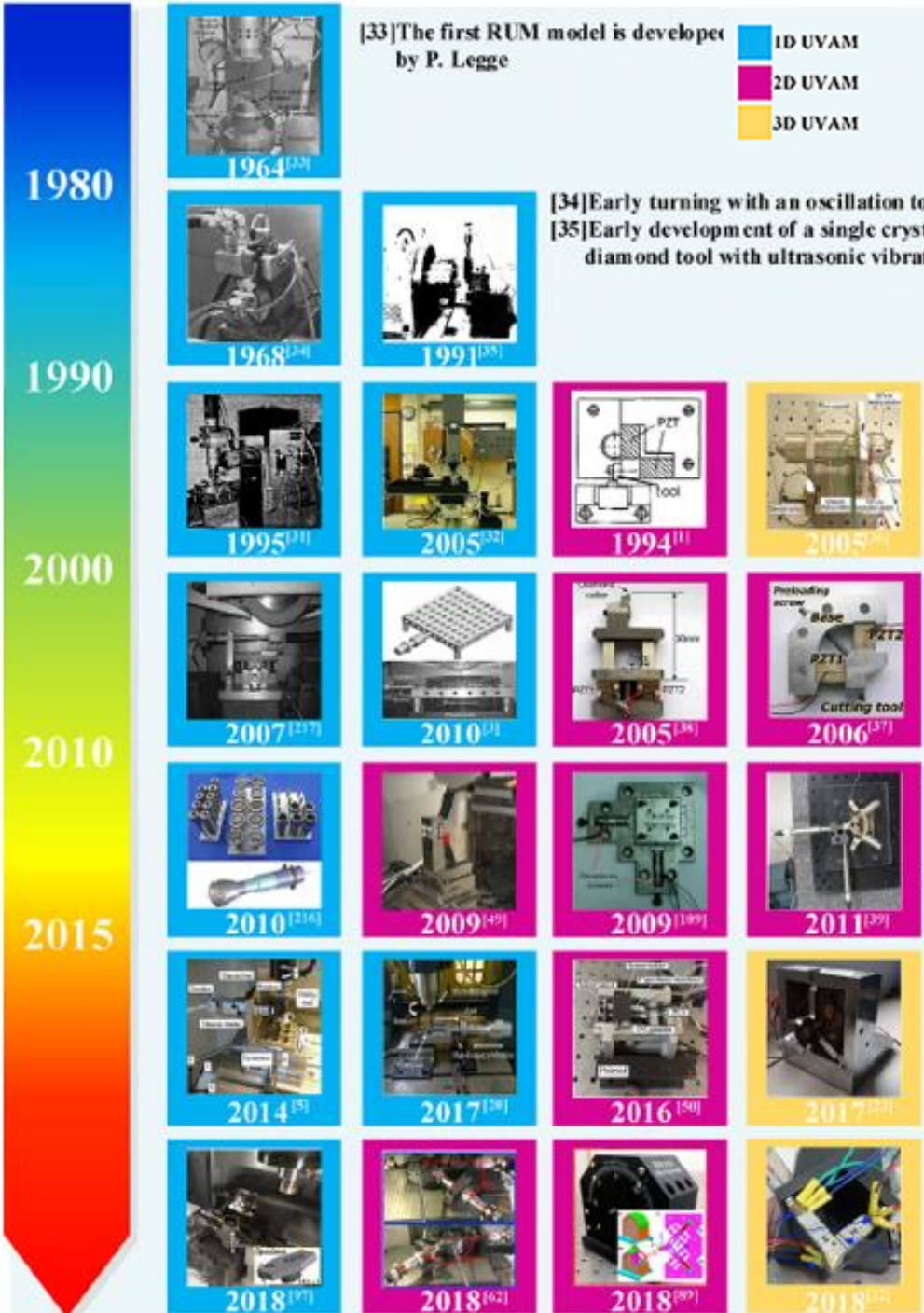


Figure 2 : Timeline of milestones in the development of UVAM [1]

After introducing VAM though general aspect, let us now observe and understand research directly related to our topic which are the improvement of surface finish through one-dimensional vibration application and the different effects thus generated while machining process compared to NVAM.

VAM is interesting for many reasons. In fact, depending on the process and how it is deployed, there are different ways to take advantage of this technology. For example, the directions of the vibrations relative to the cutting direction is a parameter which influence the surface texture and by controlling it the user can obtain Taylor-made surface patters. As mentioned by Liang-Chi Zhang [3], a wide range of applications have shown that VAM is more effective compared with its conventional process (basic cutting tool without vibration assisted). VAM physics phenomenon creates many advantages on all types of materials, including low cutting forces, long tool life, high surface integrity and excellent cutting accuracy. As explained by Liang-Chi Zhang, from brittle to ductile material, VAM improve the cutting performance. About the chip removal, a good use of the machining parameters is necessary to find an optimal configuration, by using VAM, the chip is fractured into much smaller pieces, which improved the surface integrity of the finished surface. VAM process using a cutting tool facilitate chip separation by applying an ultrasonic vibration interaction between the tool and the part which interacts at microscopic level.

It has been reported that in radial VAM on a lathe (if the vibration is performed perpendicular to the rotating axis of the workpiece) cutting forces are equal to that in conventional machining because the vibrations almost don't affect the material behaviour of the workpiece and then not change the force intensity [4]. However, in longitudinal VAM (if the vibration is done in the feed direction) the tool is separated temporarily from the sample, what evidences a reduction in the average forces compared with conventional tool, which is investigate in many studies [2]. That phenomenon also decreases the tool wear mechanisms affecting the tool.

Chen and Zheng [5] show the cutting mechanism related to vibration assisted machining compared to conventional machining. Using VAM, the material removal is not a continuous process, the vibration has a significant influence on the machining mechanism, the cutting forces are variable, and block chips are generated more efficiently. About the surface quality, VAM can reduce burr formation, which is important to obtain high quality machined surface and obtain a homogeneous and regular surface.

In recent decades, there has been an increasing demand for the surface quality and machining precision of highly sophisticated products and precision components on the machinery industry [6]. Zou [7] realised research study about surface dimensions characterisation (roughness and topography) on a steel workpiece machined with vibration assisted compared to conventional turning. It revealed that is mattered to choose appropriate process parameters which directly influence the surface quality.

The same authors shows that by using VAM, the surface quality increase related to the feed rate and depth of cut. Basically, it creates cutting marks well distributed, the space between two cutting marks is smaller, the surface become considerably symmetric and smoother. The 2D roughness obtained with assisted vibration is also significantly better.

Another interesting study carry out by Gao [8] investigate the analyse of cutting stability VAM. It explains that VAM basically improve machining quality and machining efficiency by using continuous sinusoidal vibration during machining. 2D Roughness parameters become lower using VAM. The figure 3 shows the improvement of surface quality by using vibration assisted machining, the surface amplitude become regular and smoother than conventional machining.

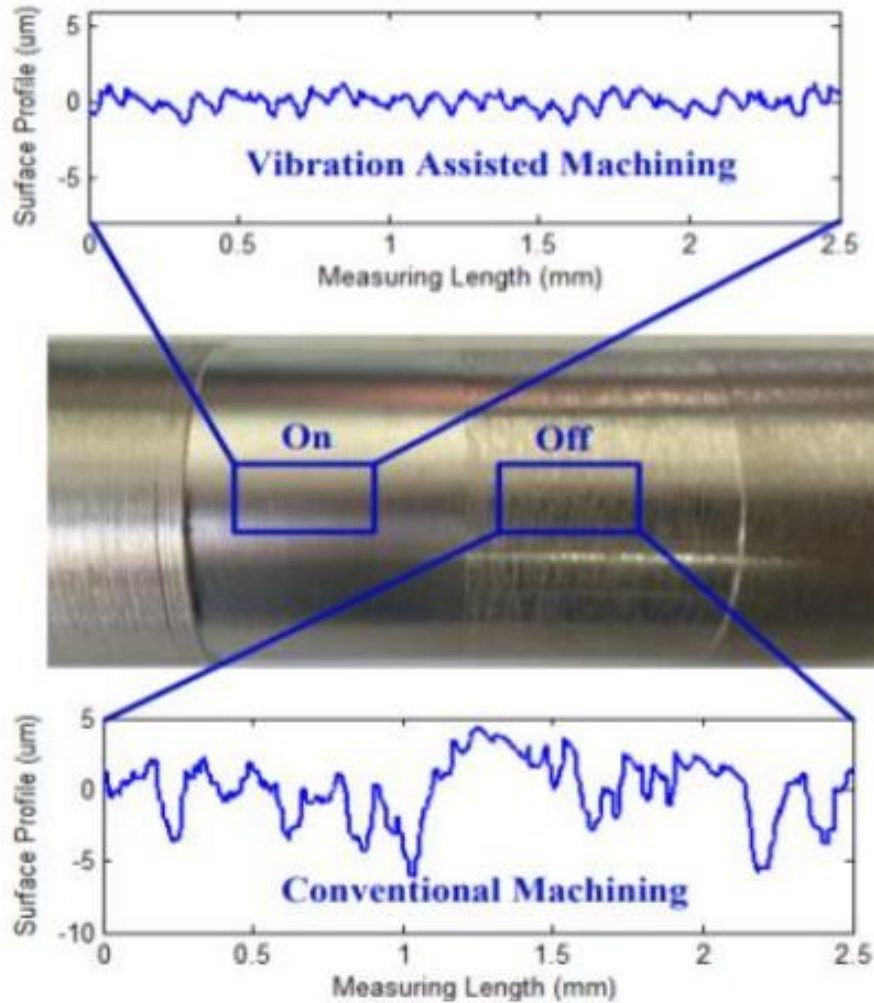


Figure 3 : Surface profile (um) depending on the machining process (VAM/conventional turning) [8]

Liu [9] propose an analyse of surface texturing in one-dimensional radial vibration assisted turning. In this study we observe the effect of processing parameters such as clearance angle, spindle speed, feed rate and vibration on the final surface texture. It is demonstrated that radial vibration assisted is an efficient way to get a specified texture surface which can be predicting by theoretical model.

Based on the current limitations and challenges described in the previous section, our research will focus on observing and characterising the effect of vibration assistance, feed and tool angle on the surface quality and cutting forces during the cutting operation. To do that, a radial VAM prototype designed by the DEFAM-TECNOFAB group will be used. As it seems that the texture is strongly influenced by radial VAM, we will analyse the texturing effect of VAM on the surface roughness and 3D texture parameters compared to conventional manufacturing. Indeed, improvement and theoretical understanding play a significant role in VAM research. Also, VAM influences the chips removal mechanism, thereby a high-speed camera will be used to characterize the vibratory effect on its formation.

3. Materials and methods

In the following section, the procedures to achieve the research objectives are described, including the experimental design, experimental setup and the materials used to conduct them. All measuring instruments to carry out the results and analysis are also described.

3.1 Experimental design

3.1.1 Ishikawa chart

First, to clearly define the limits of the experiments, an Ishikawa diagram has been done (figure 4) to define and illustrate the different aspects that define the issue that is being addressed in this master's thesis. The goal is to analyse the effect of a cutting tool assisted with vibration on the material by characterize the vibration tool effect and then obtaining the best possible manufacturing parameters in our working range. Thereby, the effect and problems observed are analysed via the chip formation, the cutting forces and via the surface quality to understand what is the characteristic surface that the tool has leaved with and without vibration. The research done in the section state-of-the-art guides us to focus on the important parameters with a real influence on the final manufacturing quality. All the parameters include in the chart below can influence the system, it can be parameters related directly to the lathe or an action resulting from previous/next step influencing the results. The causes in red are retained to perform the DOE (design of experiment).

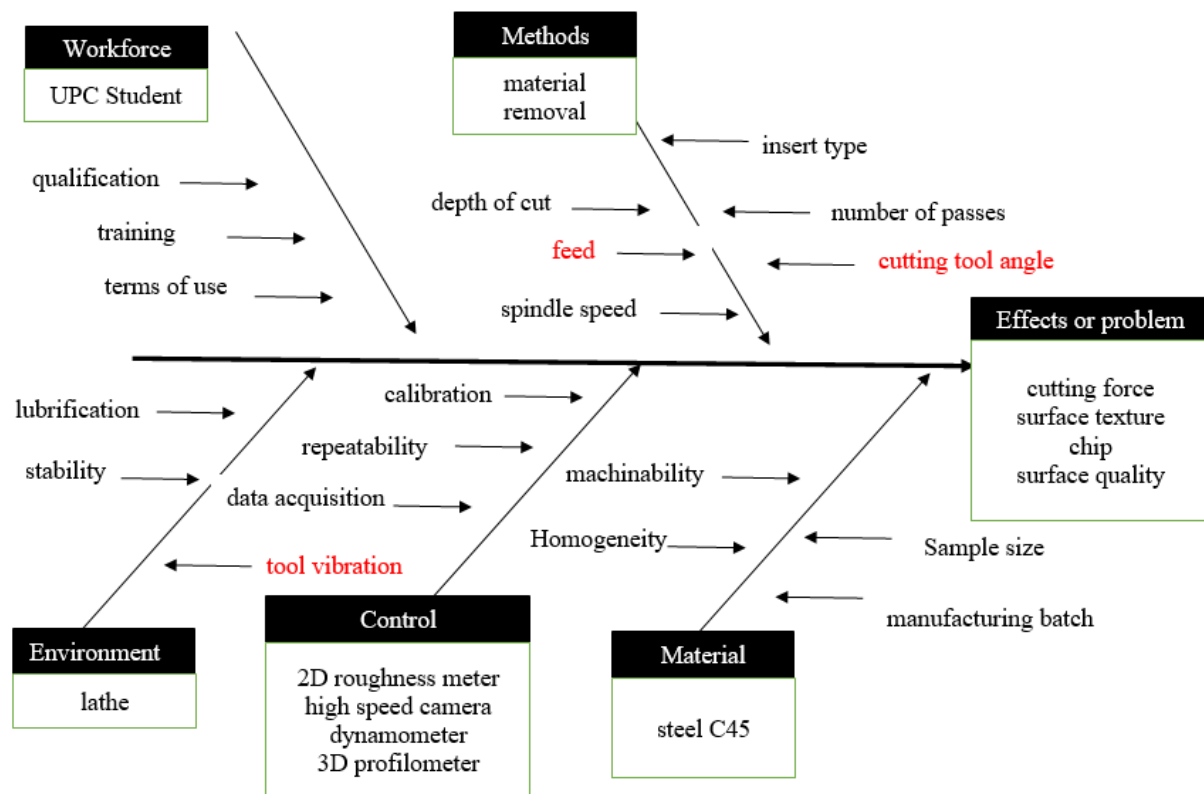


Figure 4: Ishikawa chart description

3.1.2 Experiment workflow

As the system is composed of many measurement items, the entire setup takes up a lot of space inside and around the lathe. Adapting and achieving a proper setup configuration on the conventional lathe is important to perform measurements and after different cutting operation that are relevant. To facilitate the obtention of results and adapt the experimental setup to the feasible conditions provided by the workshop and the lathe to be used, two main stages were defined to carry our research (figure 5). First, a design of experiment is defined to observe and characterise the effect of vibration assistance, feed rate and tool angle on the cutting force and surface quality during the cutting operation. Secondly, the removal chip is observed and characterised thanks to a high-speed camera. Obviously in both cases, the experiments should be realised with and without VAM to understand and analyse the effect generate on the material. On the other side, smaller experiments and assignment are realised to implement the future setups, such as determine optimal cutting speed, design and print functional part (attachment for *Kistler* and LED) and create an LED system with heat sink.

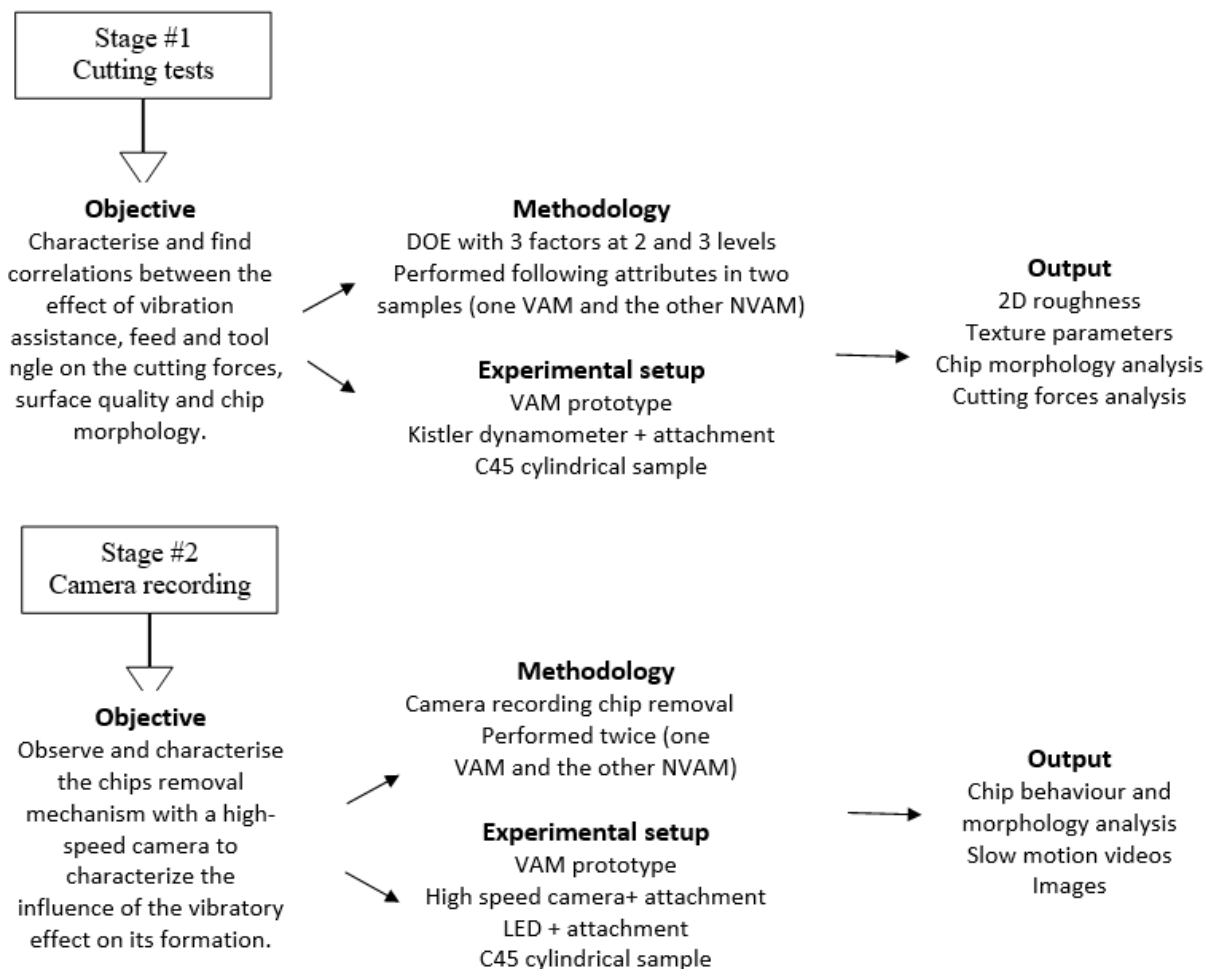


Figure 5 : Experiments workflow

3.2 Experimental setup

3.2.1 Stage #1: Cutting tests (DOE)

A design of experiments is suitable to understand and improve a manufacturing process, it helps us to investigate the effects of input variables (vibration, feed rate and tool angle KPAR) on an output variable (surface quality Ra) at the same time. DOE consist of a series of tests in which changes are generate to the input variables. Data are collected at each run, and then effects and corelations can be statistically analysed. DOE is powerful to identify the process conditions that affect quality and determine the factor settings that optimize results. Thanks to DOE, unimportant parameters can be identified. To manage and analyse data, the software *Minitab* is used. The figure 6 shows the setup used to carry out the DOE experiments. The cutting operation realised is a done with a single pass following finishing machining conditions (describe in table 2). The figure 6 shows the setup to carry out the DOE. For practical reasons, a conventional lathe is used to carry out the different experiences. A conventional lathe is a machine tool for turning parts or workpieces, where no computer is used to control the system. Lathes are available in many different designs and with every possible degree of automation. As we need to implement many stuffs such as camera, dynamometer and LED, the conventional lathe is ideal by providing many spaces and an easy way to use.

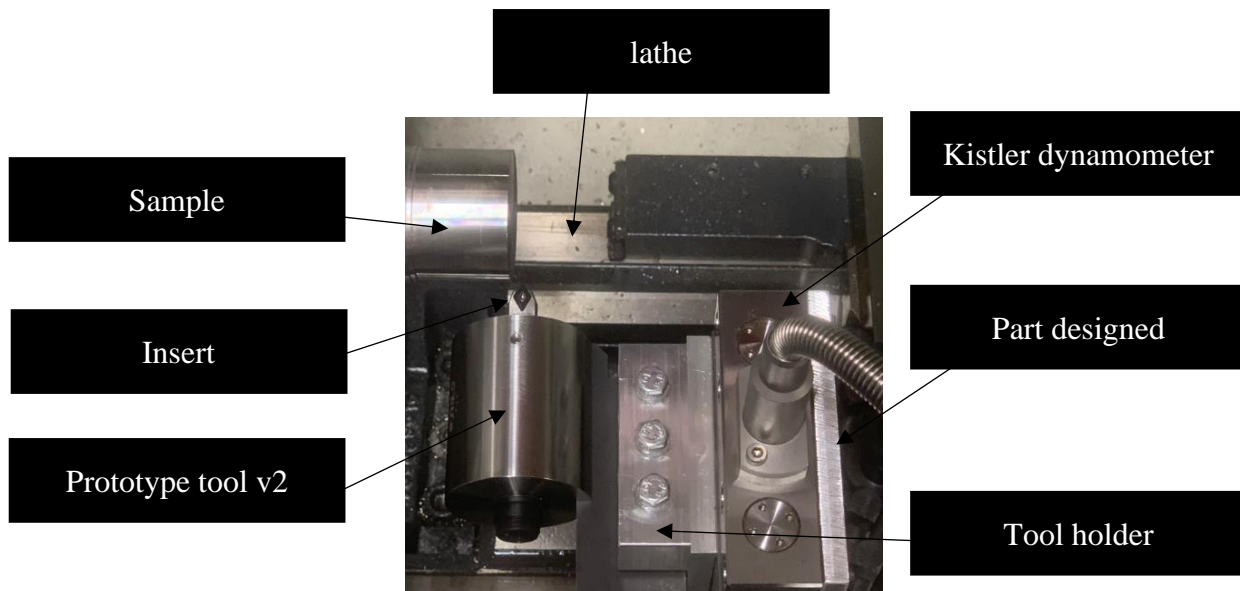


Figure 6 : Setup used to carry out the DOE experiment

Cutting experiments are conducted considering three factors at different levels. The selection of cutting parameters and their levels is define using the Ishikawa chart, state of art and knowledge from previous experiences. In our case, the DOE is achieved following the process steps of full factorial design.

To acquire force data during the machining process, a multicomponent dynamometer must be added in the lathe setup. A positioning system is already present on the dynamometer to fix the cutting tool, thereby, an intermediate part is designed for attaching the whole cutting tool system to the lathe. Here, three problematics should be considered:

- The cutting tool should be perfectly levelled and centred with the lathe rotation axis
- Limit the weight of the system while ensuring stable setup
- Limit the part dimension to avoid collisions during the machining phase

Before designing the parts, it is necessary to determine the functional dimension using two different ways to limit potential errors. A prototype obtained by 3D printing is used to validate the correct functionality of the system. After validation, the part is manufactured in aluminium to limit the weight of the system and ensure resistance to cutting forces. To acquire cutting forces during the machining process, the KISTLER 9129AA multicomponent dynamometer is used for measuring the resultant vector of the force and momentum as shown in figure 7. To acquire and control the signal, a multichannel amplifier is also used with *DynoWare* software for data acquisition.

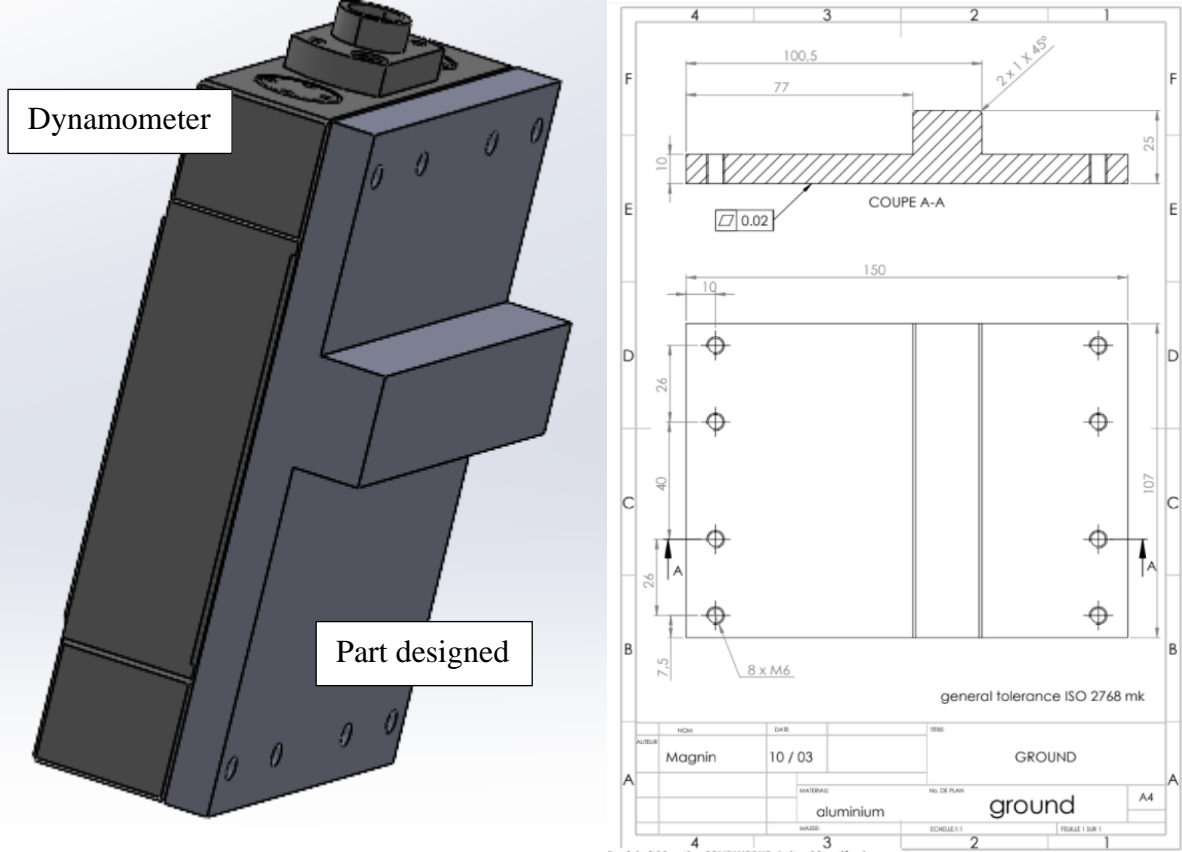


Figure 7: KISTLER 9129AA multicomponent dynamometer and part designed

Tool alignment should be carefully realised. Centre height is critical for chip control because if the cutting tool edge is not positioned correctly, the chip breaker may not provide optimal results and excessive tool wear will become an issue. Above centre causes friction and vibration, and below centre causes vibration and increased shearing zone [14]. Machine alignment is an important aspect which is regularly controlled.

Full factorial design creates experimental points using all the possible combinations of the level's factors in each complete trial or replication of the experiments are realised. The parameters study is performed following table 1.

Symbol	Factors	Level 1	Level 2	Level 3
A	Tool Vibration (kHz)	off	on	
B	Tool angle KPAR (°)	62.5	68	75
C	Feed (mm/tr)	0.07	0.1	0.14

Table 1: Factors and their level used for the DOE

D (mm)	Vc (m/min)	Ap(mm)
50	170	0.8

Table 2: Machining parameters used for the DOE

Reference	Tool Vibration (kHz)	Tool angle KPAR (°)	Feed (mm/tr)
A1B1C1	off	62.5	0.07
A1B1C2	off	62.5	0.1
A1B1C3	off	62.5	0.14
A1B2C1	off	68	0.07
A1B2C2	off	68	0.1
A1B2C3	off	68	0.14
A1B3C1	off	75	0.07
A1B3C2	off	75	0.1
A1B3C3	off	75	0.14
A2B1C1	on	62.5	0.07
A2B1C2	on	62.5	0.1
A2B1C3	on	62.5	0.14
A2B2C1	on	68	0.07
A2B2C2	on	68	0.1
A2B2C3	on	68	0.14
A2B3C1	on	75	0.07
A2B3C2	on	75	0.1
A2B3C3	on	75	0.14

Table 3: Factors and levels depending on the references

Kistler dynamometer is a sensitive measuring instrument, carefully adjusting the depth of cut between each test is very important to obtain correct and homogeny results. By increasing in the depth of cut, we increase the thickness (section) of the chip and thereby the volume of the deformed material. Due to the tool angle KPAR variation (illustrated in section 3.3.1), the radial dimension managed with the lathe should be adapted so that the effective depth of cut is kept constant at 0.8 mm throughout all experiments (figure 8).

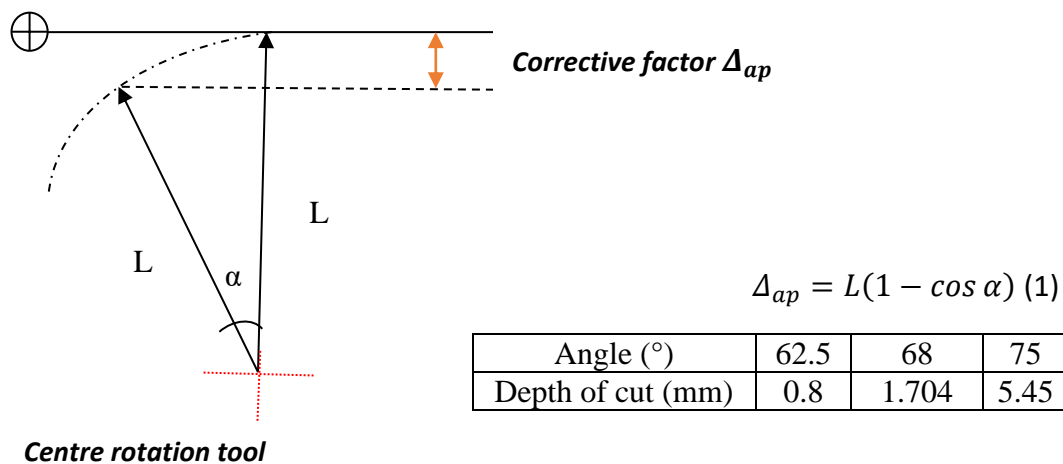


Figure 8: Depth of cut adjustment

The KISTLER 9129AA multicomponent dynamometer is used for measuring at each level the resultant force F_x , F_y and F_z corresponding to passive force F_p , the cutting force F_c and the feed force F_f , as shown in the figure. The resultant force can be determine using the equation 2.

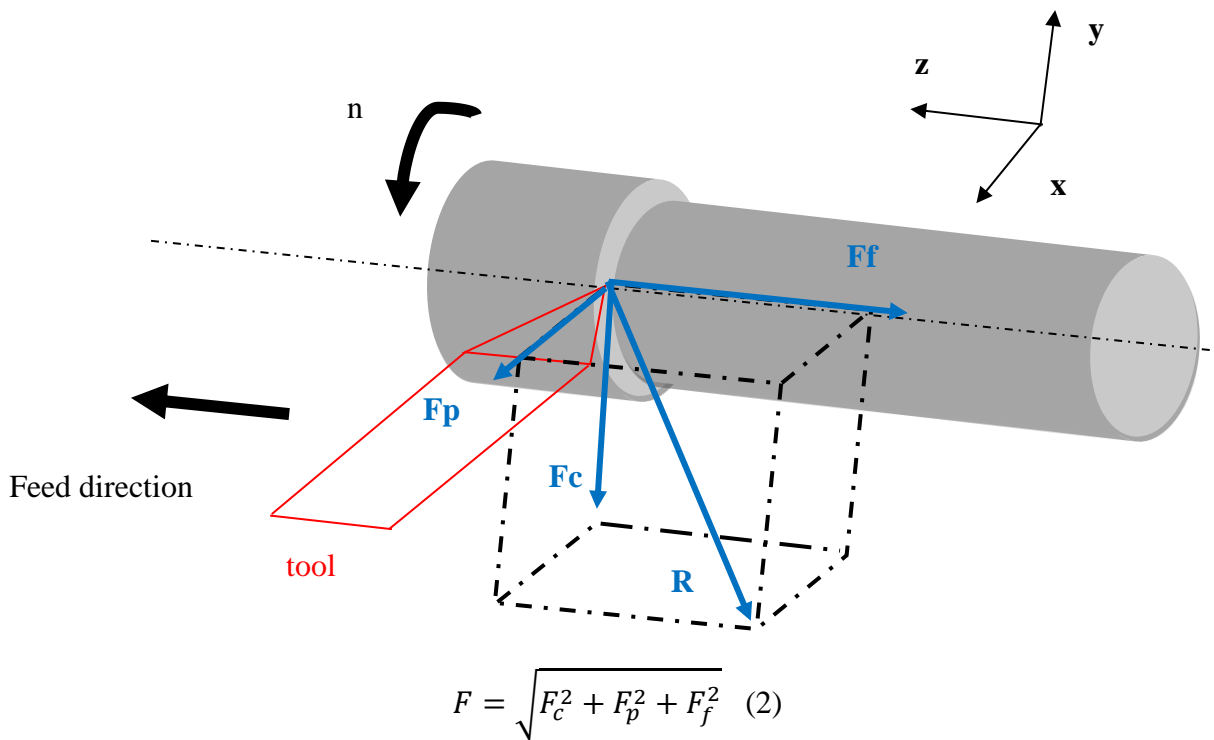


Figure 9: Cutting forces on a lathe

Limiting the modification such as angle position or depth of cut during the DOE is essential in order not to influence the results. Indeed, as shown in figure 10, eighteen combinations should be machined in the same condition to ensure results with a proper accuracy, reliability, and validity. For congestion reason (need to implement lot of experiment materials), the tailstock from the lathe cannot be used. Then the sample must be short enough to be stable and limit vibration. Thereby, two samples are defined with four manufacturing phases, each phase corresponds to a set position in the mandrel.

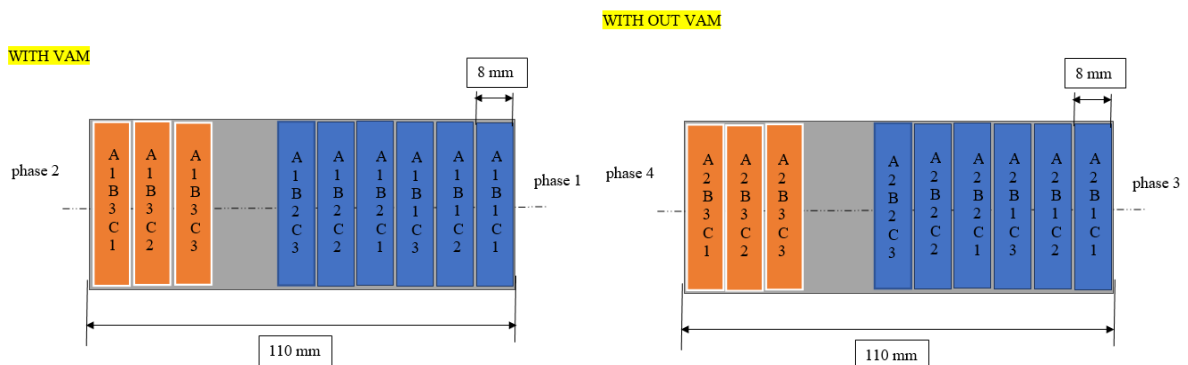


Figure 10: C45 sample with DOE references

3.2.2 Stage #2: Camera recording

Having strategies in place for controlling chips behaviour is an important part of protecting the production process, from tool life to product quality. Getting a visual behaviour of the chip breaking during the machining process gives lot of information about the smooth running of process, a regular and fragmented chip is expected to improve the tool life and the surface quality. The aim is to observe and characterise the removal chips thanks to a high-speed camera during a finishing operation with and without vibration assisted.

The high-speed camera PCO 1200 is used to carry out the experiment. Adjusting this camera is a difficult task, the focal distance should be respected to get an appropriate image (it varies according to the lens), the edge of the tool is aim. Also, there is an import balance between light absorption and reflexion. Finding a compromise between zoom, image quality and a large number of frames per second requires a huge amount of light, we are their limit by the space and the equipment used. Additive manufacturing is suitable to quickly manufacture functional parts for our system such as adjustable camera and light attachments (figure 11).

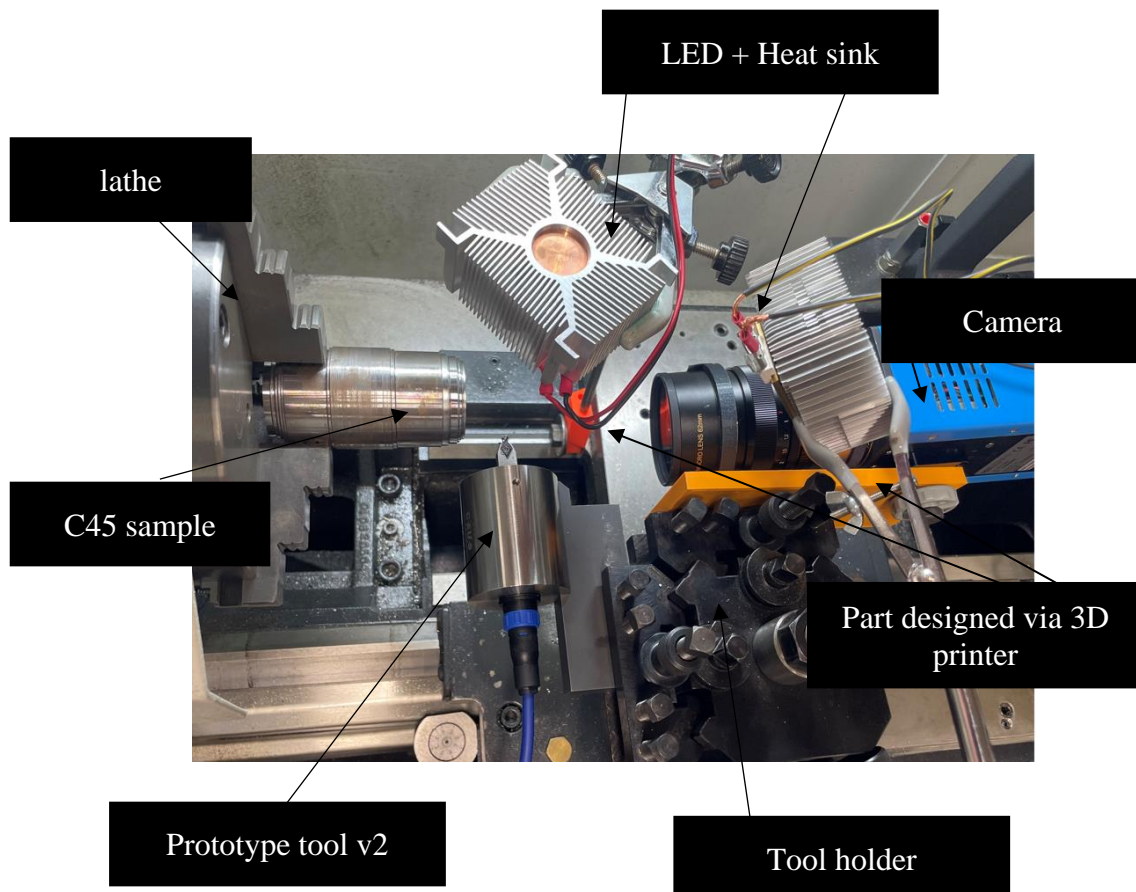


Figure 11: Camera experiment system

The PCO 1200 s high speed camera, shown in figure 12, allows us to observe the VAM effect on the removal chip. This digital camera is perfectly suited for high-speed camera application such as super slow-motion recording, inspection, or material testing. It offers a high resolution (1280 x 1024 pixel) with 486 frame per second, thereby, during the machining process the breaking chips can be visible and thus analyse. As it consists of a compact camera, it is easy setup on the lathe with an accurate adjustment. The image data are transferred via a customer selectable standard data interface to a computer, then, data can be processed. Optical lenses are also used to improve quality recording of the small area observed.



Figure 12: PCO 1200 s high speed camera

The camera cannot be used at standard light conditions. As shown in figure 11, the system is composed of two LED sources (150 W each) which should be carefully adjusted. Manage the light source and position is essential for increasing the amount of light through the camera. While recording at high frame rate, we must consider the required increase in exposure. Thereby, shooting at high frame rates requires substantial lighting levels.

To select the recording area, the ROI (region of interest) is used selecting only a part of the sensor to be read out. To setup properly the system, we start with some exposures and tries to find an exposure time that captures images with enough frame per second and proper resolution.

As indicated in the table 4, using an exposure time of 2000µs, the maximum frame rate is 367 fps. Cutting operation with and without vibration assisted are realised with the cutting parameters shown in table 5.

resolution	Exposure (us)	Rec time (s)	fps
1392 x 1040	2000	4	367

Table 4: Parameters used in the PCO software

D (mm)	Vc (m/min)	Ap(mm)	f(mm/tr)
50	170	0.8	0.1

Table 5: Manufacturing parameters used for the camera experiments

3.3 Cutting tool characteristics

3.3.1 Cutting tool configuration

The system is composed of different elements to be able to apply, control and acquire data during the machining process. Depending on the experiment carried out, the setup requires modification. For functional reasons, the cutting tool is mounted on a conventional lathe. As shown in figure 13, The toolholder give the flexibility to modify the cutting angle, as a result, the KPAR angle can vary, thereby it is a parameter to consider and evaluated during the experiments.

The Cutting tool initial position is perpendicular to the axis of rotation ($KPAR = 62.5^\circ$) and generates only radial vibrations. The initial configuration used in this study is described at figure 13.

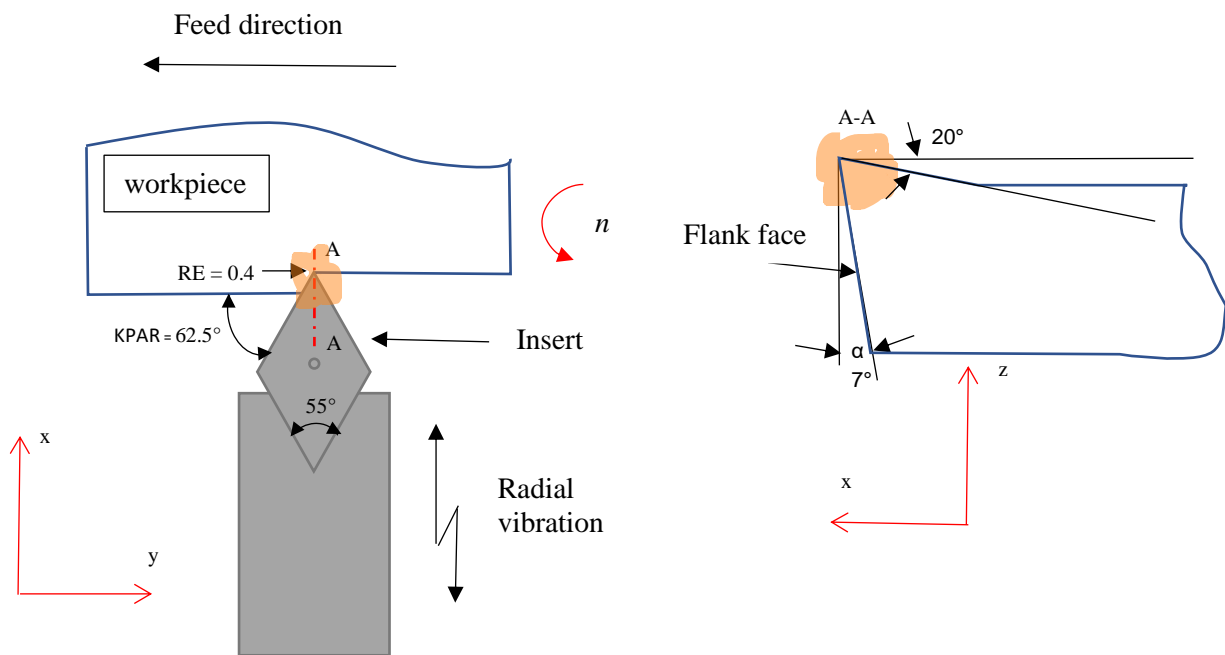


Figure 13: Cutting tool configuration and material associates

3.3.2 Prototype tool design

To conduct the experiments, the prototype shown in figure 14 was used. This vibration assisted tool works with a sonotrode which creates ultrasonic vibrations, this vibration energy is transferred to the membrane creating a vertical amplitude around $1 \mu\text{m}$. The tool body include six different parts and an ultra-high frequency connector 259PL. This prototype was designed so that the shank has a radial offset from the centre to achieve varied setup experiences on the conventional lathe.

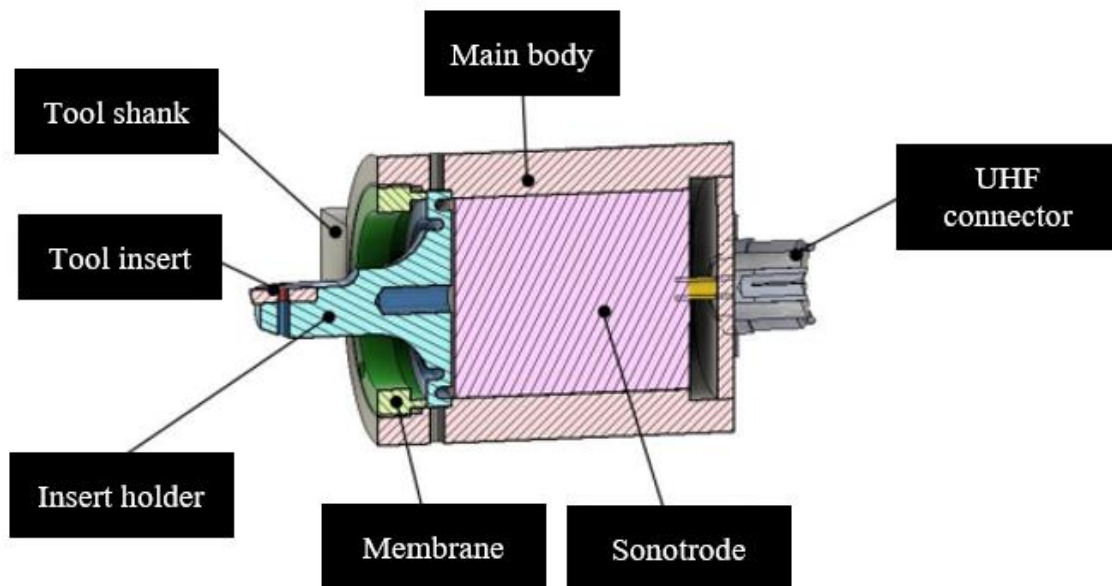


Figure 14: Prototype cutting tool V2 in section view

The main body goal is to hold most of the part together. Made in steel, it allows the assembly to remain stable and rigid to withstand cutting force. The tool shank was design to fix the cutting tool on a lathe. In our case, the tool shank is set with the dynamometer to obtain the cutting forces. Another prototype exists, the tool V1 which is designed rectangular to get more flexibility and adjustment. Both Shank and main body are made on steel. To generate the ultrasonic vibration, the sonotrode used a piezoelectric transducer attached to two metal rods. The ultrasonic frequency depends on the tool design. Both versions of the prototype, V1 and V2 resonates at a frequency of 40 kHz which create an amplitude around $1\ \mu\text{m}$. The material used to manufacture the membrane is Ti6Al4V. This keys parts generate a micrometric displacement while the resonator is active. For the experimental application in this master's thesis, the prototype V2 is used.

3.3.3 Insert type

The insert geometry was chosen in the tool design phase and based on previous experience. For finishing operation, an insert with small nose angle is preferable. A large nose angle is strong but requires more machine power and has a higher tendency for vibration. In our case, the nose angle is quite small (55°) which provide less vibration tendencies, decrease cutting forces and increase accessibility. Also, the nose radius is a keys parameter in finishing operation. A small nose radius is ideal for small cutting depth and offer better chip breaking. The tool position generates a positive turning insert which keep the clearance angle constant.

An important parameter that is studied is the entering angle, KAPR (or lead angle) which correspond to the angle between the cutting edge and the feed direction [10]. It is necessary to choose the correct lead angle for a successful turning operation because it enables the chip breaker to work correctly and avoid having continuous chips. The insert specifications are described in table 6. YG-1 DCMT070204-UF-YG3030 turning inserts design with a finishing chipbreaker. YG3030 grade is adequate for interrupted steel and stainless-steel machining [11]. It provides the highest level of wear resistance in continuous machining operations, especially in high-speed machining. YG3030, offers the optimum robustness, providing a predictable process even in the most demanding applications such as unstable conditions and interrupted machining [15]. As shown in figure 5, the insert coating is suitable for toughness material, as versatility is required in C45 steel, YG3020 is an adequate choice.

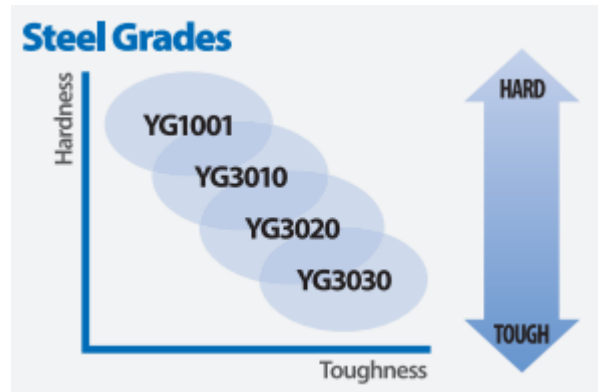
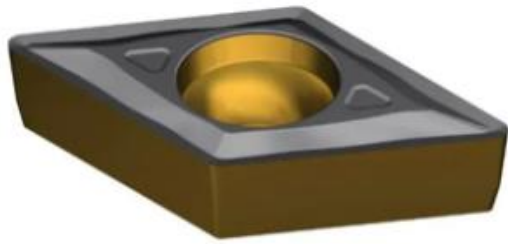


Figure 15: YG-1 DCMT070204-UF-YG3030 turning insert with a chipbreaker (source cutwell [11] and [16])

Material	Carbide
Nose angle	55°
Relief angle	7°
Rake angle	20°
Chipbreaker	UF
Corner Radius	0.4

Table 6: YG-1 DCMT070204-UF-YG3030 Turning insert relevant parameters

3.4 Materials and specimens' geometry

The material studied is a laminated bar of C45 steel which is an unalloyed medium carbon steel which is a classic carbon engineering steel. C45 is a medium strength steel which give a proper machinability and excellent tensile properties. Table 7 shows its standard composition and mechanical properties.

Steel	C	Si, ≤	Mn	S, ≤	Cr, ≤	Ni, ≤	Mo, ≤	Cr + Mo + Ni, ≤
C45(1.0503)	0.42-0.50	0.40	0.50-0.80	0.045	0.40	0.40	0.10	0.63

Property	Value	Units
Young's modulus	200	GPa
Yield strength	350-550	MPa
Tensile Strength	650-800	MPa
Poisson coefficient	0.27-0.33	-
Elongation	8-25	%
Hardness	220-260	HV

Table 7: Chemical composition and mechanical properties of C45 steel

3.5 Roughness acquisition system

Surface roughness indicates the condition of processed surfaces and play an important role in determining how a part interact with its environment such as friction. In the manufacturing industry roughness is a useful indicator of the potential performance of a mechanical component since irregularities on the surface may provide crack or corrosions.

3.5.1 Profilometer 2D

Surface topography is quantified via 2D and 3D parameters such as roughness, skewness, peak and valley distribution, etc. Measurement of these parameters contributes to better understanding of surface topography which provide useful data to characterise the effect of VAM. To carry out the 2D quality control of the sample, the 2D profilometer SJ-210 is used (figure 16), which is a portable measuring instrument that allows to measure surface roughness easily and accurately. The software can directly determine calculation results, assessed profiles, bearing and amplitude curves can be displayed. The roughness acquisition is done according to the ISO-4287 standard, which defines the properties of the surfaces, the metrology and measurement procedure parameters. In our case, the cut-off $\lambda_c=2.5$ is used regarding to the standard specification for 2D-roughness measurements.



Figure 16: 2D profilometer SJ-210

Basically, the surface based on the vertical deviations of the roughness profile from the mean line is characterize by amplitude parameters. Few of them are related to the parameters found in statistics for characterizing population samples. We describe several 2D amplitude parameters in the following table:

Parameters	Description	Formula
Ra	Average, or arithmetic average of profile height deviations from the mean line	$Ra = \frac{1}{l_r} \int_0^l z(x) dx$
Rz	Maximum peak to valley height of the profile, within a single sampling length; Average Rz value over assessment length	$Rz = B_p + R_v$
Rsk	Skewness, or measure of asymmetry of the profile about the mean line	$R_{sk} = \frac{1}{Rq^3} \left[\frac{1}{l_r} \int_0^{l_r} z^3(x) dx \right]$
Rku	Kurtosis, or measure of peakedness (or tailedness) of the profile about the mean line.	$R_{ku} = \frac{1}{Rq^4} \left[\frac{1}{l_r} \int_0^{l_r} z^4(x) dx \right]$

Table 8: 2D roughness parameters description (source 12)

3.5.2 3D surface parameters and treatment

To obtain a comprehensive 3D measuring analysis, 3D surface texture parameters are described in the flowing section according to ISO 25178 standard.

To evaluate the surface texture on the sample, the metrological device STIL Micromesure 2 3D-profilometer is used, using a white light interferometer measurement technic (non-contact measurement). This device uses light source, a camera, an objective, a mirror sport, and several beam splitters to acquire 2D or 3D roughness parameters (figure 17). To observe the surface irregularities effect, the average surface texture Sa and maximum peak Sz are defined.

The parameters Vmp, Vmc, Vvc, and Vvv are used to analyse the surface texture, they illustrate the difference between the void volume at the value p% of the area material ratio and the void volume at the area material ratio q%. The parameters Vmp, Vmc, Vvc, and Vvv show respectively the volumes of material of the eliminated peaks, of material of the clipped surface, of the void of the clipped surface and of the void of the valleys. To use the volume parameters, it is necessary to specify the surface bearing length ratios separating the eliminated peaks and eliminated valleys from the clipped surface. By default, the rates 10% and 80% are used. Indeed, two bearing ratio thresholds are defined (using the vertical bars that are drawn with dotted lines). By default, these thresholds are set at bearing ratios of 10 % and 80 % . Vvc and Vvv indicate a measure of the void volume provided by the surface between various heights as established by the chosen material ratio values. The various material volume parameters are useful to understand how much material may be worn away for a given depth of the bearing curve and how much material is available for load support once the top levels of a surfaces are worn away. The dale void volume, Vvv may be useful in indicating the potential remaining volume after significant wear of a surface has resulted. Vmp and Vmc indicate a measure of the material forming the surface at the various heights down from the highest peak of surface or between various heights as defined for Vmc [13].



Figure 17: STIL Micromesure 2 3D-profilometer

Parameters	Description	Formula
Sa	Sa is the extension of Ra (arithmetical mean height of a line) to a surface. It expresses, as an absolute value, the difference in height of each point compared to the arithmetical mean of the surface.	$Sa = \frac{1}{A} \int_0^A z(x, z) dx dy$
Sz	Sz is defined as the sum of the largest peak height value and the largest pit depth value within the defined area.	$Sz = Sp + Sv$
Sq	Sq represents the root mean square value of ordinate values within the definition area. It is equivalent to the standard deviation of heights.	$Sq = \frac{1}{A} \int_0^A z^2(x, z) dx dy$

Table 9: 3D texture parameters description (source 12)

The PSM (point sensor map) software is used to acquire the data from the 3D profilometer. Then, to manage the image rendering, the surface metrology and image analysis software Mountain is also used. Thanks to this software, we can easily get the 3D surface finish parameters and a 3D visualization of surfaces. Processing the data is an important step in order to obtain proper and correct results. Due to this sensible measuring technology irregularities or outliers can appear and distort the data. Three steps must be followed, and are explained in detail in the annex:

- Select an area where there are no irregularities caused by measurement
- Flatten the shape (measuring a cylindrical surface)
- Adjust the axes and the image properties in an adequate range

4. Results and analysis

4.1 Preliminary tests: determination of optimal Vc

To facilitate the experimental process, the optimal cutting velocity is determined previously and use as a basis to conduct the two following experiments (DOE and camera recording). As the cutting velocity determined is theoretical, it matter to use it as a starting point and then vary it in a close interval according to the machining conditions to observe the influence on the surface quality. This carbide inset is ideal to machine unalloyed steel. The cutting speed V_c , depth of cut ap and feed are given by the insert supplier in a wide range. The cutting speed recommended for an unalloyed steel is between 70 - 350m/min. The depth of cut corresponds to the depth of engagement of the tool in the part, for finishing operation $ap = 0.5 - 2\text{mm}$. However, V_c should be refined as it can vary following the material, the tools used, insert coting, and the type of operation. The feed f is the movement in millimetres of the tool during one revolution of the part. This is also the thickness of the chip, the surface finish (grooves) and the machining time are directly related to the feed f . The formula (3) express the spindle speed which depends on the cutting velocity and the sample diameter, the values obtained are set in the lathe parameter before each machining operation.

$$n = \frac{vc \cdot 1000}{\pi \cdot d} \quad (3)$$

n : rotation frequency rpm)

vc : cutting speed (m/min)

π : constant π

d : diameter of the tool for milling and diameter of the part of revolution for turning (mm)

Vc (m/min)	f(mm/tr)	Ap(mm)
70 - 350	0.05 - 0.2	0.5 - 2

Table 10: Manufacturing parameters from the supplier

D (mm)	f(mm/tr)	Ap(mm)
54.8	0.1	0.8

Table 11: Manufacturing parameters used for the camera experiments

Rpm	Vc	\bar{R}_a	σ	\bar{R}_q	σ	\bar{R}_z	σ	\overline{Rsk}	σ	\overline{Rku}	σ
800	138	1.316	0.20	1.436	0.05	6.800	0.40	-0.048	0.16	2.363	0.1
900	155	1.165	0.05	1.447	0.07	7.513	1.14	-0.170	0.24	2.689	0.78
1000	172	1.164	0.05	1.413	0.08	7.013	0.68	-0.031	0.11	2.422	0.23
1100	189	1.369	0.09	1.735	0.10	8.586	0.95	-0.325	0.19	2.538	0.84
1200	206	1.354	0.20	1.497	0.16	7.965	1.65	-0.090	0.07	2.560	0.05
1300	224	1.510	0.34	1.871	3.17	10.521	3.17	0.234	0.38	3.028	1.2

Table 12: Results from the optimal Vc experiments



Figure 18: the arithmetical mean deviation of the roughness profile (Ra) depending on the cutting velocity

All the values described above (table 12) are the average of three measurements to increase reliability, the standard deviation is used to measure the dispersion of a set of values around their mean. Lower is the standard deviation, more homogeneous is the population.

It is expected to be a minimum as the adequate value for the arithmetical mean deviation of the roughness profile (Ra). As shown in figure 18, Vc around 170 (m/min) is optimal providing an average of Ra= 1,164 µm which is clearly satisfying for a finishing operation. On the other hand, the further away from this value, more Ra increases with a similar trend for the standard deviation. To carry out this experiment, a new insert is used and thus generate high-quality surface but a sensible behaviour from the roughness response. Indeed, due to the insert wear following a Taylor model, the design of experiment (next section) is realised with a slightly degraded insert, providing a stable behaviour with acceptable repeatability even the surface quality deriving from the insert state is weaker.

The values of the maximum height of the roughness profile (Rz) are also considered in our relevant amplitude parameters. Around Vc 170 (m/min), we get as an average Rz=7.013 µm as well as a minimum value with a small standard deviation which gives confidence in our result.

In addition, Rsk and Rku are useful parameters to describe the surface distribution, it demonstrates the peakedness and abruptness of the surface. In all cases the Skewness Rsk is lightly negative, an ideal value of Rsk should be around 0, at Vc 170 (m/min), Rsk is the closest to 0 which means a homogeneity and smooth shape. Kurtosis explains the distribution sharpness, all the Vc values provide a surface quality with a kurtosis value close to 3 which correspond to a surface profile of Gaussian distributions. In our case, Rku < 3 which means that the surface profile has relatively few high peaks and low valleys which is probably due to the feed rate (creating the grooves profile).

4.2 Stage #1: Cutting tests

4.2.1. Influence of DOE factors on roughness results

Sample	\bar{R}_a	σ	\bar{R}_q	σ	\bar{R}_z	σ	\overline{Rsk}	σ	\overline{Rku}	σ
A1B1C1	3.108	0.02	3.761	0.08	18.013	0.52	0.467	0.01	2.574	0.11
A1B1C2	1.676	0.05	2.050	0.04	10.414	0.24	0.010	0.15	2.490	0.12
A1B1C3	2.236	0.19	2.745	0.25	14.457	2.42	0.072	0.12	2.599	0.33
A1B2C1	2.211	0.06	2.930	0.06	13.446	0.54	1.387	0.59	2.671	0.46
A1B2C2	1.968	0.20	2.520	0.31	11.873	0.94	0.451	0.86	2.882	0.51
A1B2C3	1.760	0.02	2.186	0.08	11.320	0.94	-0.011	0.34	2.932	0.22
A1B3C1	3.125	0.05	3.676	0.06	14.727	0.18	0.250	0.09	1.940	0.06
A1B3C2	3.019	0.17	3.442	0.05	16.239	1.02	0.367	0.49	3.703	0.23
A1B3C3	1.731	0.02	2.109	0.01	10.850	0.86	0.041	0.04	3.177	0.19

Table 13: Results from the DOE without vibration (A1)

Sample	\bar{R}_a	σ	\bar{R}_q	σ	\bar{R}_z	σ	\overline{Rsk}	σ	\overline{Rku}	σ
A2B1C1	2.314	0.16	2.907	0.08	12.487	0.88	0.110	0.10	2.199	0.12
A2B1C2	1.569	0.02	1.941	0.04	10.073	0.60	0.107	0.10	2.725	0.18
A2B1C3	2.020	0.04	2.503	0.09	13.668	1.35	-0.118	0.39	2.811	0.44
A2B2C1	1.784	0.08	2.217	0.10	11.799	0.86	0.246	0.25	2.582	0.31
A2B2C2	1.612	0.07	1.989	0.12	9.994	1.05	-0.018	0.07	2.621	0.23
A2B2C3	1.491	0.10	1.852	0.11	10.050	0.44	0.527	0.36	2.840	0.24
A2B3C1	1.873	0.41	2.291	0.47	11.373	1.66	0.129	0.08	2.316	0.19
A2B3C2	1.641	0.03	2.059	0.07	11.448	1.66	0.017	0.22	2.966	0.45
A2B3C3	1.807	0.08	2.191	0.11	11.190	0.74	0.097	0.16	2.602	0.31

Table 14: Results from the DOE with vibration (A2)

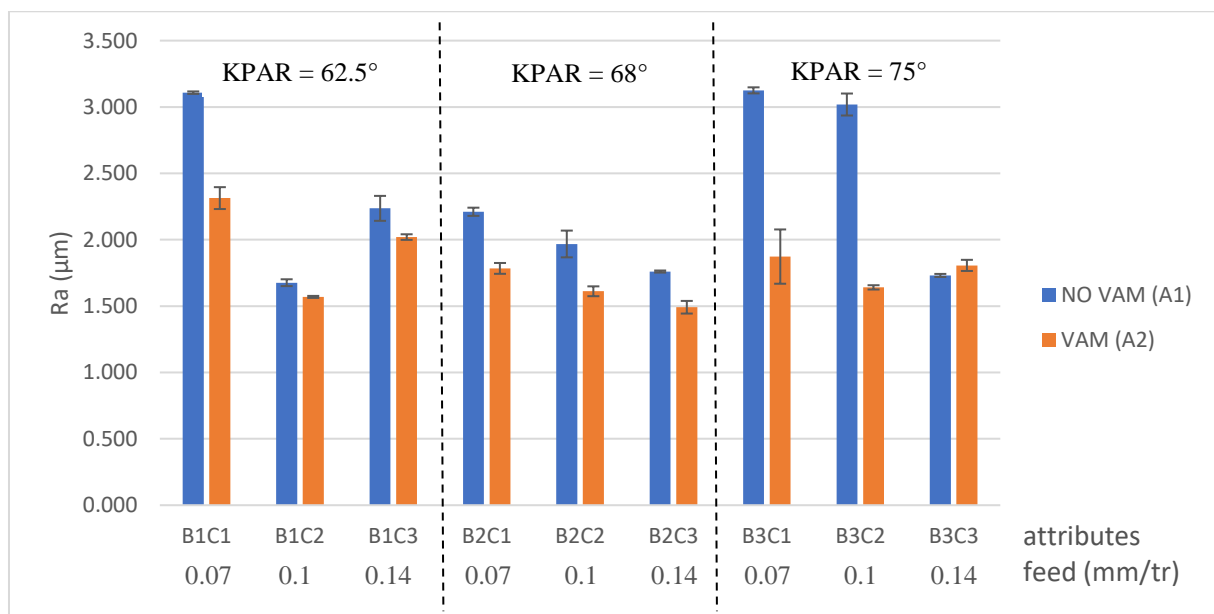


Figure 19: Arithmetical mean deviation of the roughness profile (Ra) depending on the attribute

As the previous experiments, all the values described above are the average of three measurements to increase reliability, the standard deviation is used to measure the dispersion of a set of values around their mean. The arithmetical mean deviation of the roughness profile (Ra) is used as the response for the DOE. Both table 13 and 14 show the relevant parameters from the 2D profilometer.

The figure 19 shows the arithmetical mean deviation of the roughness profile (Ra) depending on the attribute. From a global point of view, it is undeniable that adding vibration to the tool decreases the value of Ra which means a proper surface finishing quality. Only the combination B3C3 gives a Ra value lower without using vibration, both values are close one from the other and have a large standard deviation, which suggests that these two values can be the same. To investigate the cause of this phenomenon, a chip analysis is carried out in the following section. To go deeper into the analysis, *Minitab* results such as residual plots, main effect and interaction are used. Ra values obtained previously are in an acceptable range related finishing operation. As explain in the previous experiment, the insert used is lightly worn to get stable results, which provides globally lower surface quality compared to section 4.1.

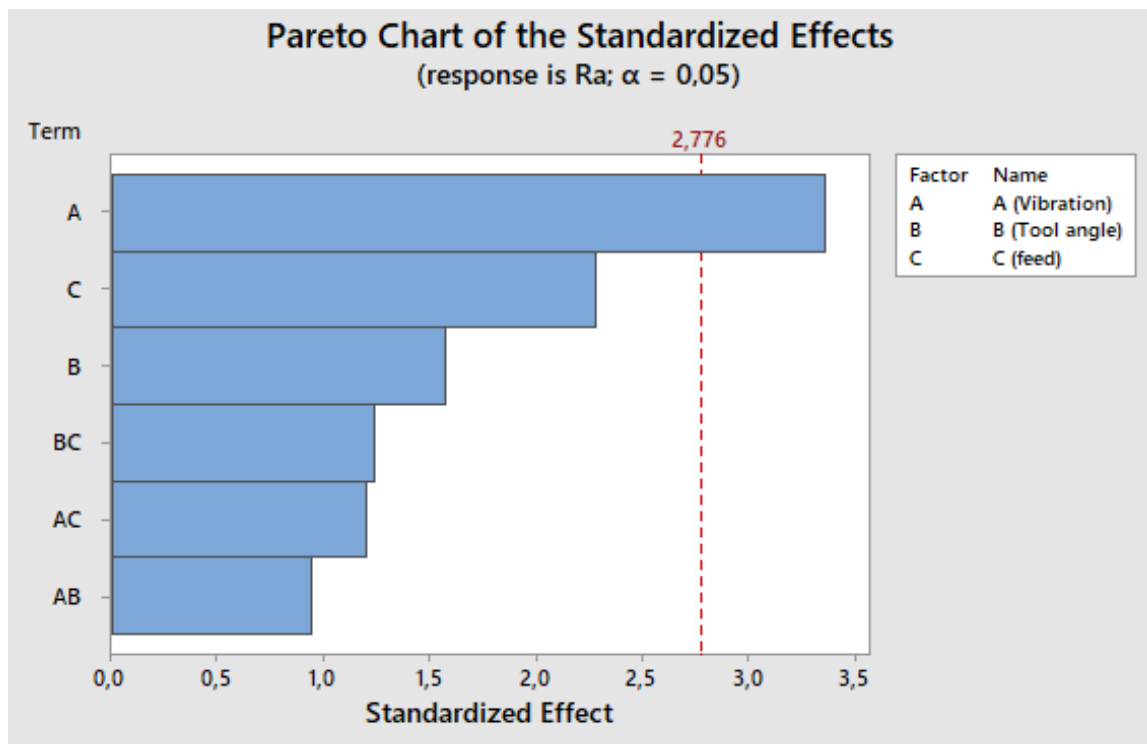


Figure 20: Pareto chart of the standardized effects response Ra

The Pareto chart gives information about the factors and interactions having significant impact on the response. From the figure 20, almost all factors and interaction are below the dotted line, from a statistical point of view, only the vibration add to the tool has a significant influence regarding to the arithmetical mean deviation of the roughness profile (Ra). We must keep in mind that the vibration effect probably hides the effects of the other two factors and also that from the three levels explored, the insignificant difference found between them could be only observed between two of them, but not with the third one. For this reason, a complete graph of the mean effects is represented below.

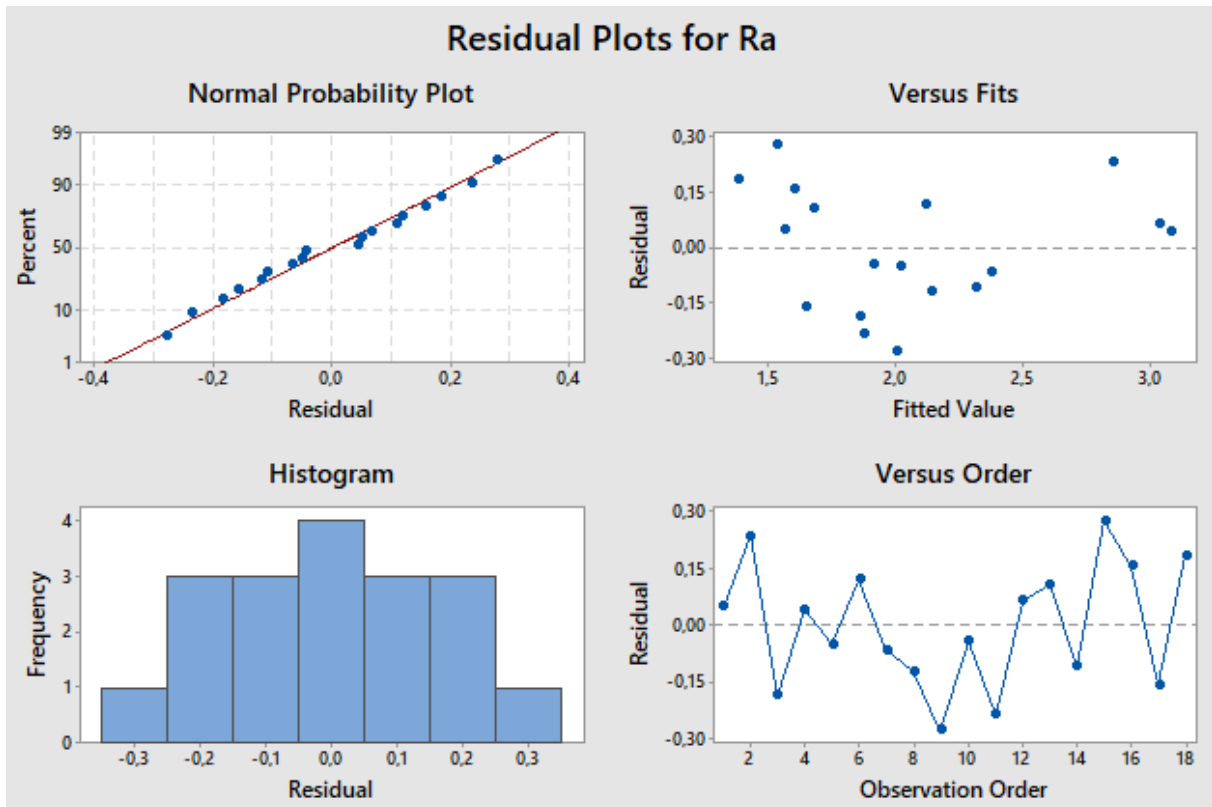


Figure 21: Residual plots for Ra

The figure 21 shows the residual plots which correspond to the differences between real experiment values and predictions based on the model. The software *Minitab* gives four different ways to represent the residuals, it seems clear that these residuals are normally and randomly distributed. About the normal probability plot, the residuals approximately follow a straight line which mean that the residual are normally distributed. The residual histogram is useful to determine whether the data are skewed or include outliers. In our case, the histogram is perfectly symmetric, corresponding to a normal distribution. The residuals depending on order plot shows the residuals in the order that data are collected. No pattern is detected in this chart, which means that the residuals are independent from one another. All these information supports the validity of the results.

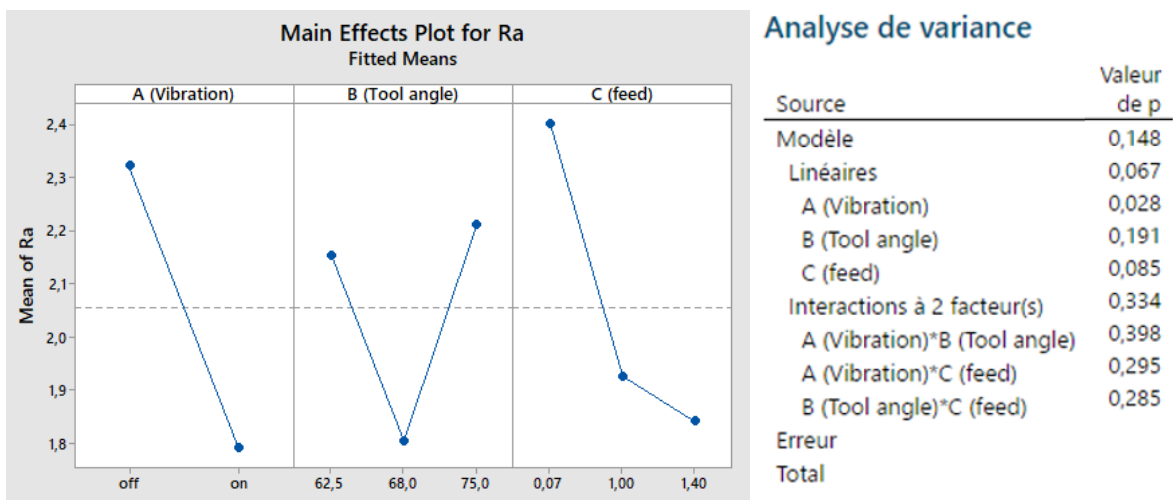


Figure 22: Main effects plot for Ra and P values

The main effects plot is suitable to investigate differences between level means for one or more factors. A main effect is detected when different levels of a factor affect the response differently. The figure 22 illustrate the main effect for vibration, tool angle and feed depending on the response Ra.

From this chart, many aspects should be considering for conducting a proper and correct analyse. Basically, when the line is not flat (horizontal), a main effect may be detected. The steeper the slope of the line, the greater the magnitude of the main effect. However, it matters to take into account the *P value* which gives an indication of the probability that the results are different or statistically equivalent. From a general point of view, the vibration is the most significant effect on Ra providing lower value than without vibration assisted machined. For the vibration factor $P = 0.028$, as *P*-value is traditionally compared to α values of less than 0.05, it indicates at a significance level of 0.05, the mean values of Ra are significantly similar from the observed values.

About the tool angle, $KPAR = 68^\circ$ seems to minimize the Ra while the two other tool position generate higher values. For this parameter, the interval plot and *P* values are used to support the validity of this analyse (figure 22). For the tool angle, the mean values with superimposed confidence intervals means that we cannot conclude on the difference or not of the mean Ra at a level of 62.5, 68 and 75. Also, *P*-value = 0.191 which means that at a significance level of 0.05, the mean Ra related to the tool angle values seems to be significantly different from the observed values. Thereby, these means values can probably be the same from a statistical point of view. To refine the difference, more measurements of the three level must be carry out.

About the feed rate, Ra seems to be lower (decreasing trend) while increasing the feed. The first slope (between 0,07 – 0.1) is steeper than the second iteration which probably means that increasing the value of KAPR has more effect between 0.07 – 0.1 than 0.1 – 0.14. From the interval plot (figure 23), as the previous case, the mean values with superimposed confidence intervals means that we cannot conclude on the difference or not of Ra mean values at a level of 0.07, 0.1 and 0.14. *P* value = 0.085 which means that at a significance level of 0.05, the mean Ra related to the tool feed rate is significantly different from the observed values.

However, the *P* value remains close to the significance level of 5% which suggests that feed stay an important parameter. Obviously, the feed influences the quality surface, processing the combination of these 3 factors highlights the effect of vibration and probably hide the feed effect. The feed keeps playing a crucial role in the surface quality; indeed, lathe machining often provides a groovy surface creating from the feed rate marks.

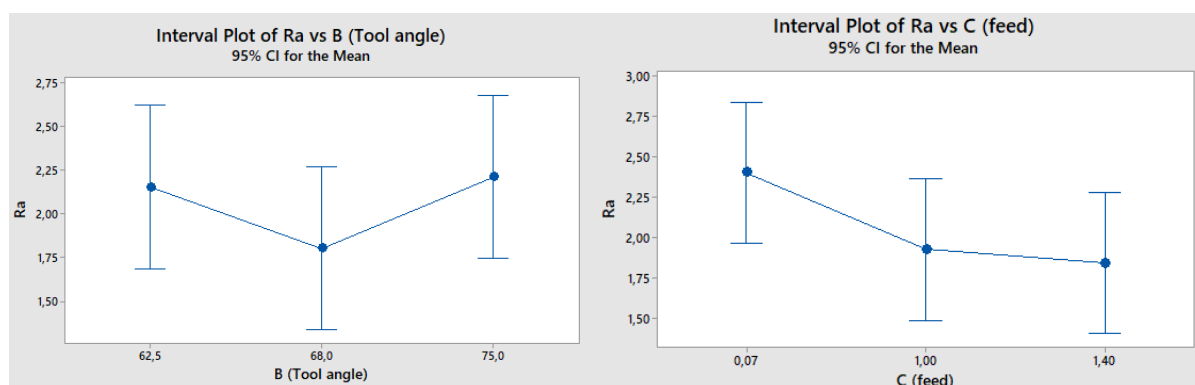


Figure 23: Interval plot for tool angle and feed rate

The figure 24 shows the interaction plot which helps to determine the influence of one categorical factor on the relationship between a second categorical factor and a continuous response Ra. The lines illustrate the influence of the interactions on the relationship between the factors and the response. If the lines are parallel, there is no interaction, in the opposite way, when the lines are not parallel or crossing, there is an interaction. The less the lines are parallel, the stronger the interaction. There are three cases where there are crossed lines on the graph which suggest that there is an interaction effect. As the previous analysis, by looking at the p-value (figure 22), the interaction term is not statistically significant. As an example, in the interaction vibration*tool angle, the green and blue lines (related to tool angle values) are crossing. However, the green dot at a level vibration “on” is probably different from the observed value, which means that the lines are not crossing and thus define no interaction in all cases.

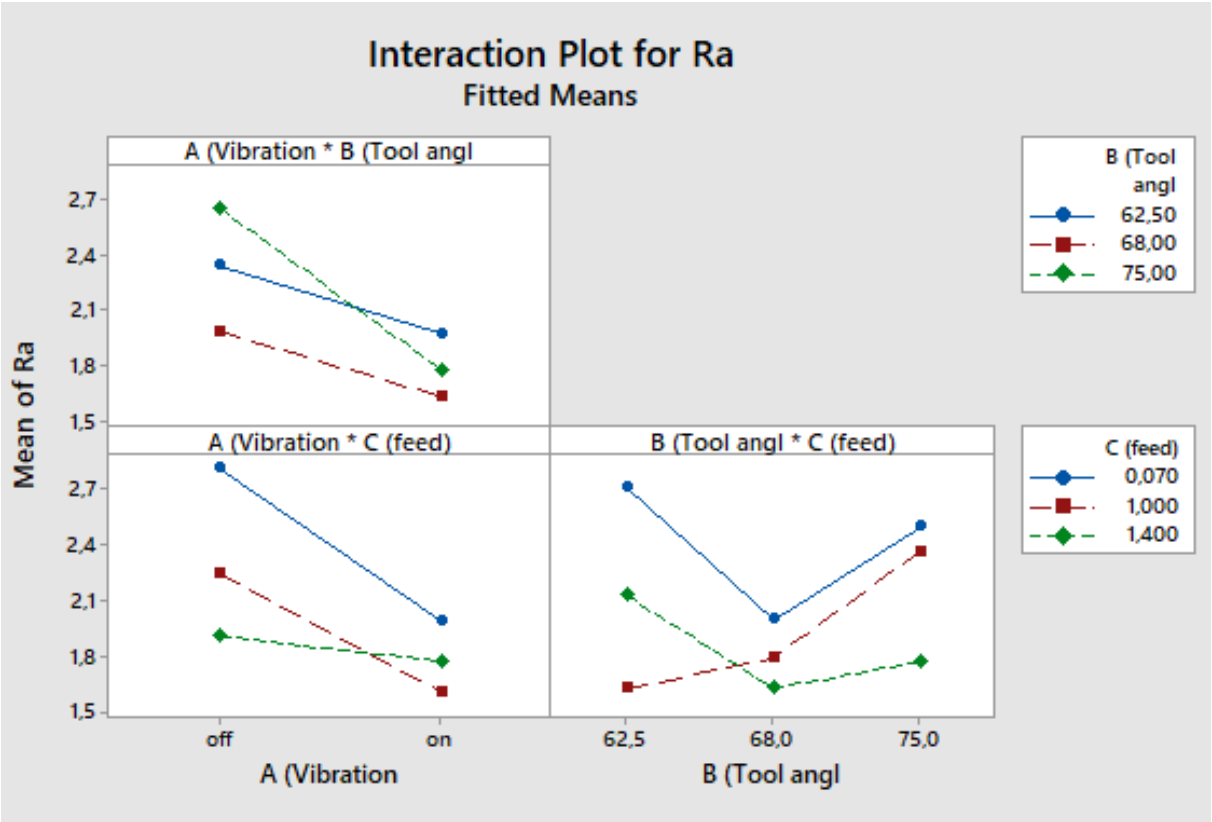


Figure 24: Interaction plot for Ra

Minitab software is suitable for quality improvement. The DOE study has clearly indicated that full factorial design is an effective method for understand and analyse the VAM effect. By using a higher number of tests, we could reduce the P value and refine the validity of the results. It matters to be very careful with the analysis of the charts results.

4.2.2. Influence of DOE factors on cutting forces

The KISTLER 9129AA multicomponent dynamometer forces is used for measuring at each level the resultant force F_x , F_y and F_z corresponding to passive force F_p , the cutting force F_c and the feed force F_f . As illustrate in the figure 9 (section 3.2.1), the resulting force can be determine using the equation (2). The figure 25 shows the different forces depending on the factor combination (only feed rate and tool angle are considering). All the values described below are the average of three measurements to increase reliability, the standard deviation is used to measure the dispersion. As explored in the section state of art, the cutting force are equivalent with and without applying vibration, this phenomenon can be observed on the figure 26, which shows no forces variation in the two cases from a macroscopic point of view.

In addition to a large standard deviation, as shown in the figure 27, the measurements have a significant noise which increases with feed rate increment. All these phenomena generate a sensitive result analysing. It is necessary to take into account the fact that the study concerns a finishing operation phase, which means that the factors variation is weak, and thereby cannot necessarily be observable via the Kistler dynamometer.

F_x (pushing force) remains globally constant considering the wide standard deviation, due to a fixed value of the depth of cut. About the cutting force F_c (F_y) and the feed force F_d (F_z), a small variation is identified following a rising trend while increasing the feed rate (easily identifiable on the feed force). It makes sense that the highest forces are the vertical cutting force due to removal material process. F_c depend on K_c (daN/mm²) which is the specific cutting pressure, this parameter is related to the chip thickness, the workpiece material, the depth of cut (in mm) and the feed rate f (mm/tr) .

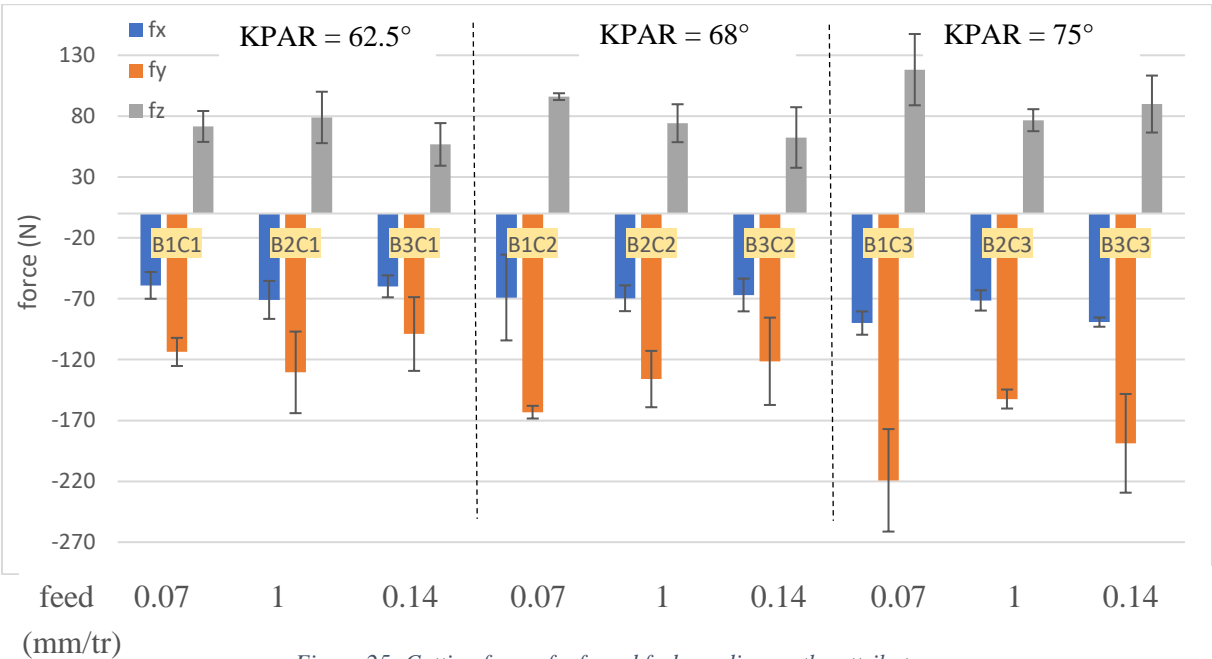


Figure 25: Cutting forces f_x ; f_y and f_z depending on the attribute

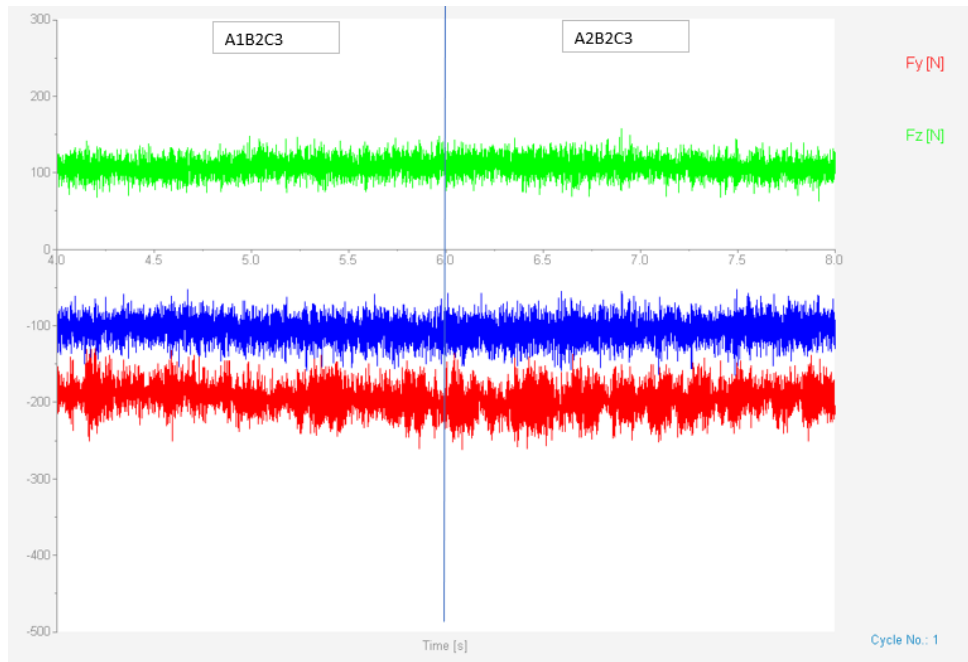


Figure 26: Cutting forces f_x ; f_y and f_z of attribute B2C3 with and without vibration

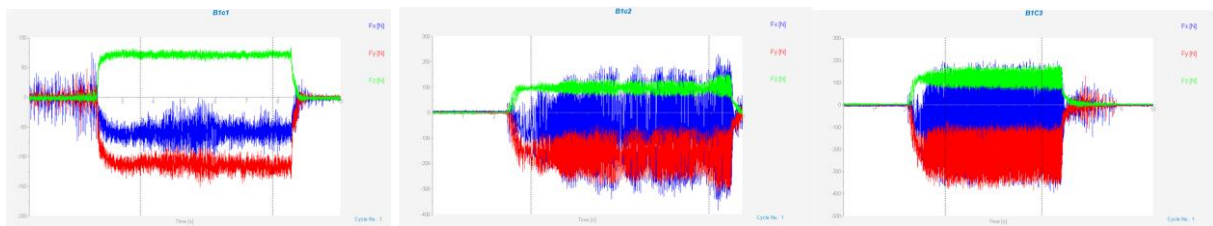


Figure 27: Cutting forces f_x ; f_y and f_z amplified with feed rate increasing

The figure 28 shows the fast Fourier transform (FFT) which is a computationally efficient method of generating a Fourier transform. The fast Fourier transform translate the waveform from the Kistler signal into a frequency spectrum to decipher the exact frequency that exists in this recording. The goal here is to identify the noise origin. Two main peaks are identified, corresponding at $f=200$ Hz to the lathe working frequency and at $f=5000$ Hz to a pump present in the basement. As the floor of the workshop is not coating, the exterior vibration probably influences the results measuring from the Kistler. We were expected to observe the ultrasonic vibration frequency from the tool, as the Kistler acquisition is macro, it is impossible to observe this phenomenon via the FFT chart.

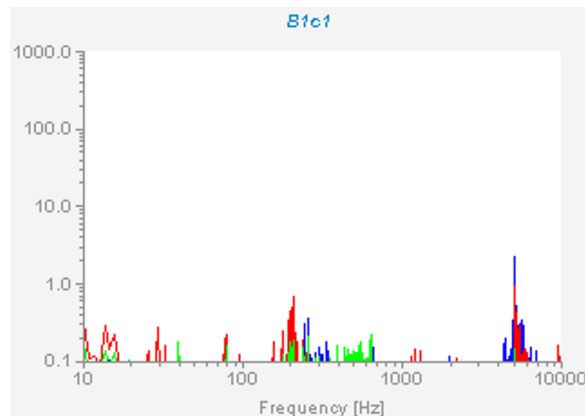


Figure 28: Cutting forces f_x ; f_y and f_z expressed with Fourier transform

4.2.3. Influence of DOE factors on chip formation

During the DOE process, all the chips are picked up and then analysed based on the standard ISO 3885 (annex page 50). The chip formed during the finishing cutting operation has characteristics related to many parameters such as work material, cutting edge and tool geometry. As the insert used a chipbreaker, the chip is expected to be broken in order to get a proper quality surface and improve tool life. When machining materials, long and continuous chips can be not properly evacuated, then the tool edge risks rapidly to be worn or deteriorate. The curled chip can wrap around the workpiece or tool, its evacuation becomes delicate and dangerous, and then has a significant effect on the surface quality.

The table 15 shows the chip characteristics related to the factors combination. Four different families of chips are identified (described and analysed in the following section), the arithmetical mean deviation of the roughness profile (Ra) is also shown as the response to analyses the influence of chip formation on the surface finish.

sample	chip state	chip form	Ra
A1B1C1	continuous	Tubular long / Snarled	3.108
A1B1C2	continuous	Tubular long / Snarled	1.676
A1B1C3	semi continuous	Tubular long	2.236
A1B2C1	continuous	Tubular snarled	2.211
A1B2C2	continuous	Tubular snarled	1.968
A1B2C3	semi continuous	Tubular short	1.760
A1B3C1	continuous	Washer type long / snarled	3.125
A1B3C2	continuous	Tubular snarled	3.019
A1B3C3	breakage	Arc chips loose	1.731
A2B1C1	continuous	tubular snarled	2.314
A2B1C2	breakage	Arc chips loose / connected	1.569
A2B1C3	breakage	Arc chips loose	2.020
A2B2C1	continuous	tubular snarled	1.784
A2B2C2	breakage	Arc chips loose	1.612
A2B2C3	breakage	Arc chips loose	1.491
A2B3C1	breakage / continuous	Arc chips loose / snarled	1.873
A2B3C2	breakage	Arc chips loose	1.641
A2B3C3	breakage	Arc chips loose	1.807

Table 15: Chips results from the DOE

The chip formation influences the manufacturing quality, Indeed, as shown in figure 29 , the arithmetical mean deviation of the roughness profile (Ra) remains higher while the chips is continuous. On the other hand, when a fragmented chip is obtained, the value of Ra tends to be lower. A spinning continous chip risks to damage the machined surface, and may be difficult to evacuate towards the chip trays

All the continuous chip formation (blue line) belongs to level C1 or C2 which means a lower feed rate, thereby, a higher feed rate helps chip breakager. Even if a low feed is often advised for the finishing operation, it is important to ensure a feed rate large enough to obtain a fragmenting chip. Most level combination with vibration cause a chip breakage, only B1C1 and B2C1 provide continous chip due to the weak feed rate C1 (0,07 mm/tr) which is clearly not adaqueate even with or without vibration assited. The angle variation KPAR seems to have a weak influence on the chip formation. For the same combinaison, adding vibration caused a fragmentation of the chip which is really relevant. Indeed , by applying vertical amplitude vibration , the tool comes in and out the material which improves chip breakage mechanism.

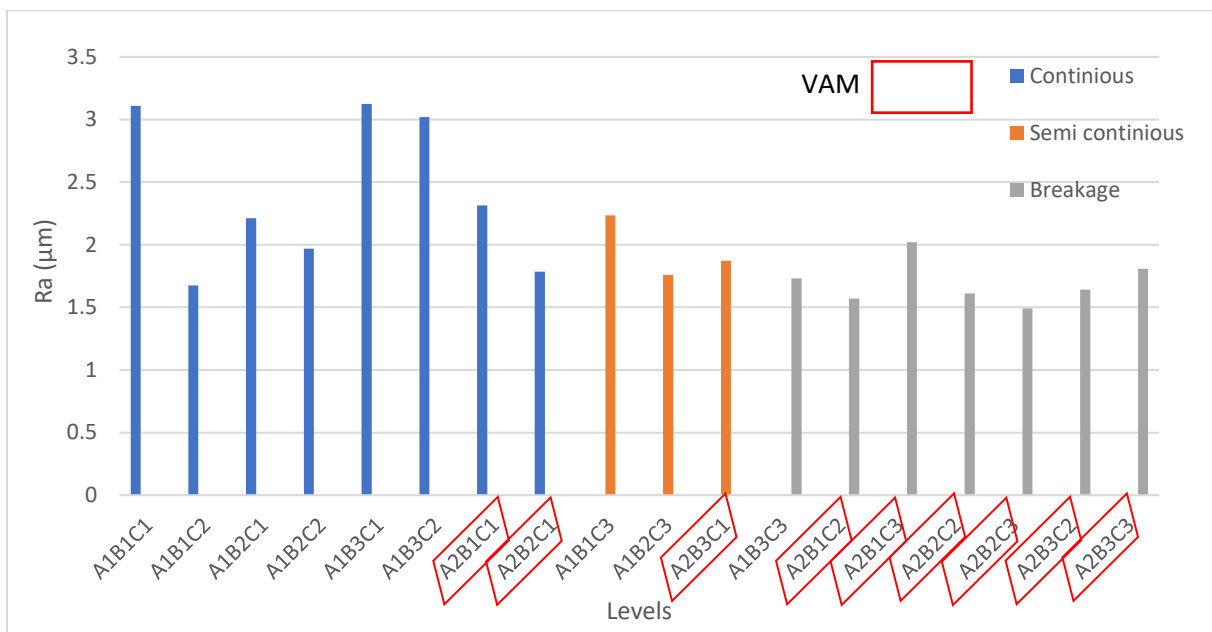


Figure 29: The arithmetical mean deviation of the roughness profile (Ra) depending on the attribute

Both following table give visual aspect of the chips formation after machining depending on the feed rate and the tool angle. By looking at the figure 29, it seems clear that increasing the feed rates generates proper chip from tubular long/ snarled to arc chip loose shape. From the figure 30 (without VAM), only the feed rate corresponding to C3 gives fragmented chips.

All the factors combination from C1 and C2 are inadequate, the cheap is snarled which risks to damage the machined surface by friction due to poor evacuation of the chip. From the column B3, the tool angle seems to have an effects on the chip formation. Indeed, by increasing the tool angle KPAR from B1 to B3, the chip becomes considerably fragmented following the state continuous, semi continuous and breakage as shown in figure 29 . This phenomena shows that while using a higher feed rate, the tool angle KPAR start to have a stronger effect on the chip formation.

A1	C1 f=0.07 (mm/tr)	C2 f=0.1 (mm/tr)	C3 f=0.14 (mm/tr)
B1 62.5°			
B2 67°			
B3 75°			

Figure 30: Chips image from the DOE regarding level combination (attribute) without vibration

For the same level combination, adding vibration assisted machining clearly provide better cheap formation. As show in the figure 31, almost all combination generates arc chip loose, which improve surface quality by looking at the Ra value (table 15). By looking at both figure 30 and 31, applying vibration helps the chipsbreaker to work propely and generates mainly arc chip loose. Even adding vibration, the feed rate C1 provide snarled chip which create an higher Ra value as shown in table 15. As the effect of vibration seems to strongly affect chip formation, the tool angle effect is weaker and probably hide by the vibration factor. The factor combination, at level of A2B2C3 provide the greater surface quality Ra = 1.491 um and a regular breaking chip.


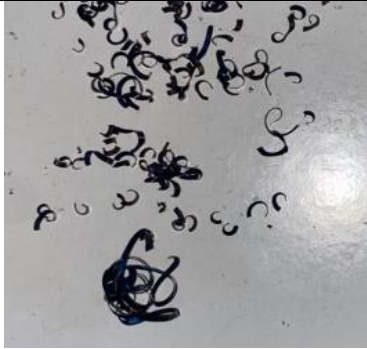



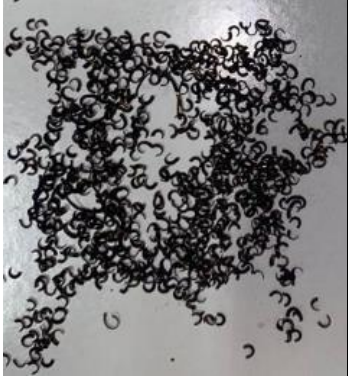



A2	C1 f=0.07 (mm/tr)	C2 f=0.1 (mm/tr)	C3 f=0.14 (mm/tr)
B1 62.5°			
B2 67°			
B3 75°			

Figure 31: Chips image from the DOE regarding level combination (attribute) with vibration

4.2.4. Influence of DOE factors on texture parameters S and V

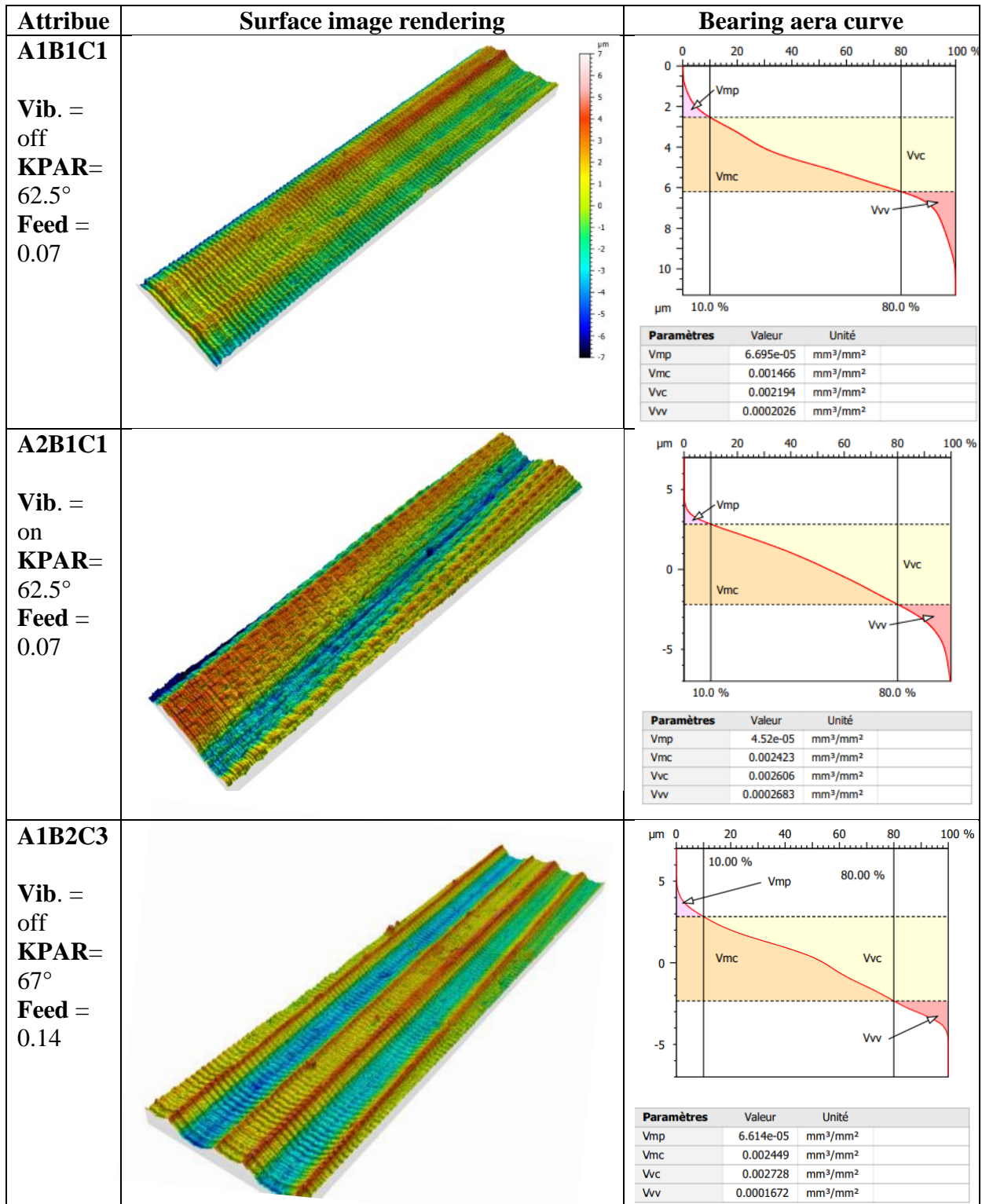
attribute	Sa [μm]	Sq [μm]	Sz [μm]
A1B3C3	1.783	2.169	12.32
A2B3C3	1.835	2.272	16
A1B2C3	1.899	2.206	11.29
A2B2C3	1.524	1.822	11.29
A1B1C1	2.93	3.43	70.83
A2B1C1	1.976	2.357	16.84

Table 16: 3D roughness parameters

In the following section, the main relevant results found via 2D roughness are analysed using 3D profilometer to understand and observe the parameters effects on 3D texture. From the previous analysis, B2C3 is the most appropriate combination to obtain a proper surface quality (2D roughness). Another interesting combination is the B3C3 which is the only case where Ra vibration > Ra without vibration. Finally, level B1C1 seems to provide the worst surface quality regarding 2D roughness profile, which can be interesting to observe and characterise compared to B2C3.

The parameters Sa, Sq and Sz (describe in section 3.5.2) are used to characterise the surface. As shown in table 16, following the same logic than the 2D results, the combination B2C3 provide the lower average Sa and root mean square roughness Sq which means the micro-irregularities on the surface texture are weak. The attribute at level B1C1 is not a suitable compromise, a lower feed rate seems to generate a texture with more form defect and irregularities. Vibration seems to be the most influential factor that affects surface texture since surface deteriorates without applying vibration. As the previous analysis via 2D roughness, the level B3C3 gives lower Sa without vibration than with but both values are close and then can be identical.

To describe the texture deeply and analyse the micro irregularities, the table 17 shows the visual surface aspect and the bearing area curve. Graphical study of volume parameters Vmp, Vvc, Vmc, and Vvv (explained in section 3.5.2) based upon the Abbott curve are useful to describe the surface texture. Indeed, for each combination applying vibration significantly modify the deep void volume Vvv and the pick material volume Vmp which directly influence the material ability to resist friction or wear. It seems clear that by increasing the feed rate and tool angle, the effect of vibration become stronger forming higher valley and picks. This phenomenon is easily observable on combination B3C3, no vibration generate only deep grooves create by tool insert related to the feed rate. Applying vibration add valley though the grooves generate by the vertical amplitude from the tool. From VAM to NVAM, two different patterns are easily observable (A1B3C3 = linear shape; A2B3C3 = mesh shape). The pattern intensity seems to depend on the feed rate, higher the feed rate is, more visible is the pattern. KPAR angle effect is considerably weaker but seems to amplify marks. About the A1B3C3, Vvv is widely superior to Vmp which means that the surface contains mainly valley (gorge) as shows in the 3D texture image corresponding. Having an adequate balance between Vmp and Vvv influences the surface quality. Indeed, as show combining both table 16 and 17, for getting the lowest Sa (most appropriate surface quality), Vmp should be equal or close to Vvv in order to obtain an homogenous flat surface, as seen 3D texture image A2B2C3 (Vibration = on; KPAR = 68°; f = 1.4 mm/tr).



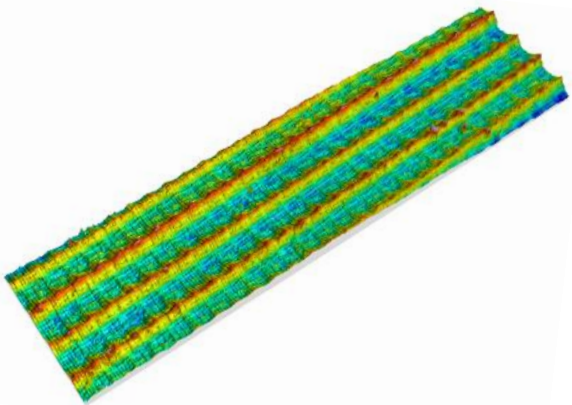
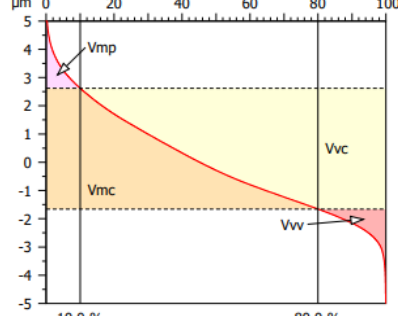
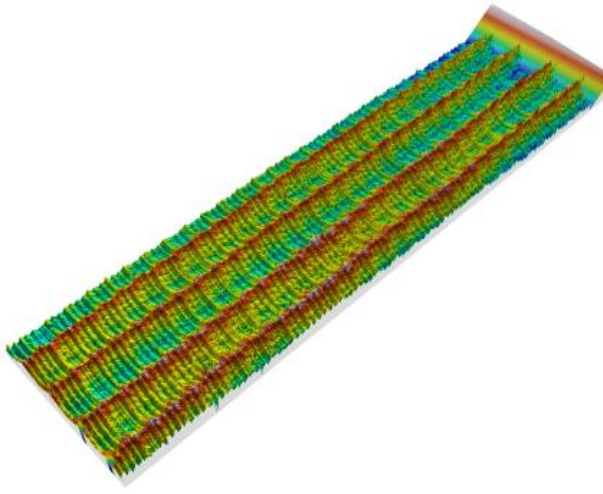
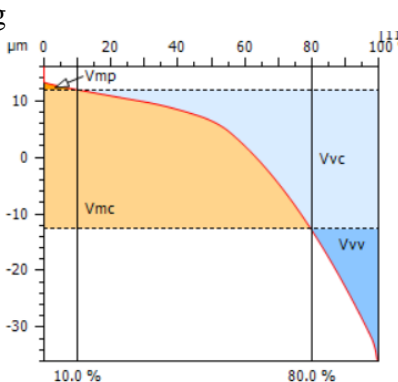
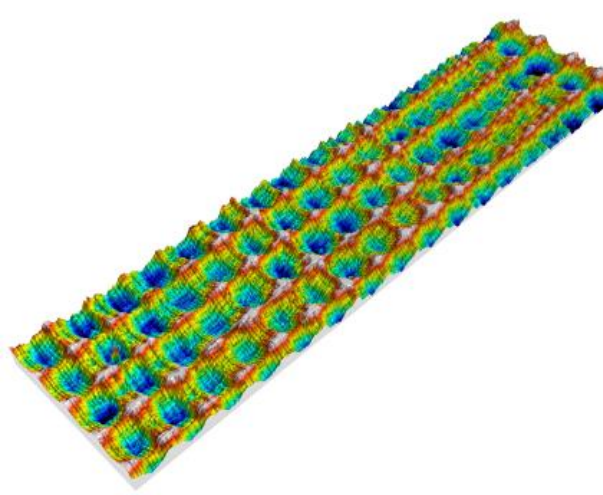
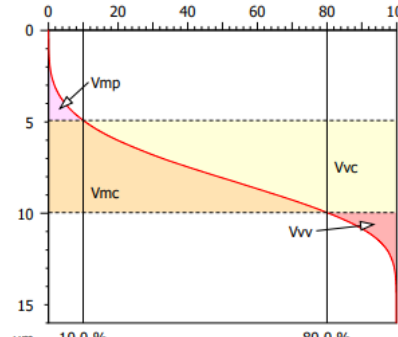
<p>A2B2C3</p> <p>Vib. = on KPAR= 68° Feed = 0.14</p>		 <table border="1"> <thead> <tr> <th>Paramètres</th> <th>Valeur</th> <th>Unité</th> </tr> </thead> <tbody> <tr> <td>Vmp</td> <td>8.239e-05</td> <td>mm³/mm²</td> </tr> <tr> <td>Vmc</td> <td>0.001703</td> <td>mm³/mm²</td> </tr> <tr> <td>Vvc</td> <td>0.002575</td> <td>mm³/mm²</td> </tr> <tr> <td>Vvv</td> <td>0.0001282</td> <td>mm³/mm²</td> </tr> </tbody> </table>	Paramètres	Valeur	Unité	Vmp	8.239e-05	mm ³ /mm ²	Vmc	0.001703	mm ³ /mm ²	Vvc	0.002575	mm ³ /mm ²	Vvv	0.0001282	mm ³ /mm ²
Paramètres	Valeur	Unité															
Vmp	8.239e-05	mm ³ /mm ²															
Vmc	0.001703	mm ³ /mm ²															
Vvc	0.002575	mm ³ /mm ²															
Vvv	0.0001282	mm ³ /mm ²															
<p>A1B3C3</p> <p>Vib. = off KPAR= 68° Feed = 0.14</p>		 <p>Information</p> <p>Réglage du filtre: Sans filtrage.</p> <table border="1"> <thead> <tr> <th>Paramètres</th> <th>Valeur</th> <th>Unité</th> </tr> </thead> <tbody> <tr> <td>Vmp</td> <td>6.039e-05</td> <td>mm³/mm²</td> </tr> <tr> <td>Vmc</td> <td>0.01468</td> <td>mm³/mm²</td> </tr> <tr> <td>Vvc</td> <td>0.009915</td> <td>mm³/mm²</td> </tr> <tr> <td>Vvv</td> <td>0.002049</td> <td>mm³/mm²</td> </tr> </tbody> </table>	Paramètres	Valeur	Unité	Vmp	6.039e-05	mm ³ /mm ²	Vmc	0.01468	mm ³ /mm ²	Vvc	0.009915	mm ³ /mm ²	Vvv	0.002049	mm ³ /mm ²
Paramètres	Valeur	Unité															
Vmp	6.039e-05	mm ³ /mm ²															
Vmc	0.01468	mm ³ /mm ²															
Vvc	0.009915	mm ³ /mm ²															
Vvv	0.002049	mm ³ /mm ²															
<p>A2B3C3</p> <p>Vib. = on KPAR= 75° Feed = 0.14</p>		 <table border="1"> <thead> <tr> <th>Paramètres</th> <th>Valeur</th> <th>Unité</th> </tr> </thead> <tbody> <tr> <td>Vmp</td> <td>0.0001091</td> <td>mm³/mm²</td> </tr> <tr> <td>Vmc</td> <td>0.002099</td> <td>mm³/mm²</td> </tr> <tr> <td>Vvc</td> <td>0.002945</td> <td>mm³/mm²</td> </tr> <tr> <td>Vvv</td> <td>0.0002153</td> <td>mm³/mm²</td> </tr> </tbody> </table>	Paramètres	Valeur	Unité	Vmp	0.0001091	mm ³ /mm ²	Vmc	0.002099	mm ³ /mm ²	Vvc	0.002945	mm ³ /mm ²	Vvv	0.0002153	mm ³ /mm ²
Paramètres	Valeur	Unité															
Vmp	0.0001091	mm ³ /mm ²															
Vmc	0.002099	mm ³ /mm ²															
Vvc	0.002945	mm ³ /mm ²															
Vvv	0.0002153	mm ³ /mm ²															

Table 17: Visual aspect and bearing area curve

4.3 Stage #2: Camera experiment

The following figures illustrate the visual behaviour of the chip during the machining process with and without vibration. Both experiments are realised with the same cutting condition shown in figure 9. The challenge related to this experiment was correctly adjusting the camera to get a propre image (as explained in section 3.2.2). For both configuration (with and without VAM), the images are processed and generated according to the parameters show in the following table 18.

The figure 32 shows the machining operation without vibration, at $t=0.5$ s the chips is continuous generating a tubular long shape. A spinning continious chip risks to damage the tool insert, and is difficult to evacuate towards the chip trays. Few seconde later, at $t=1.7$ s, the chip start to wrap around the tool which is sensitive to the surface quality. Indeed, its evacuation becomes delicate and dangerous, provinding heat and friction.

Oppositely, as shown in figure 33, the chip is fragmented and evacuated in the right direction (chip tray) which ensures no damage on the tool insert or on the machined workpiece. The tool amplitude is too weak (around $1 \mu\text{m}$) to be observed on the images. It is difficult to observe the chip evacuation due to the focal distance set on the edge of the tool.

Resolution	Aspect	Time between frames (s)
720 x 576	color	0.002

Table 18: image processing parameters

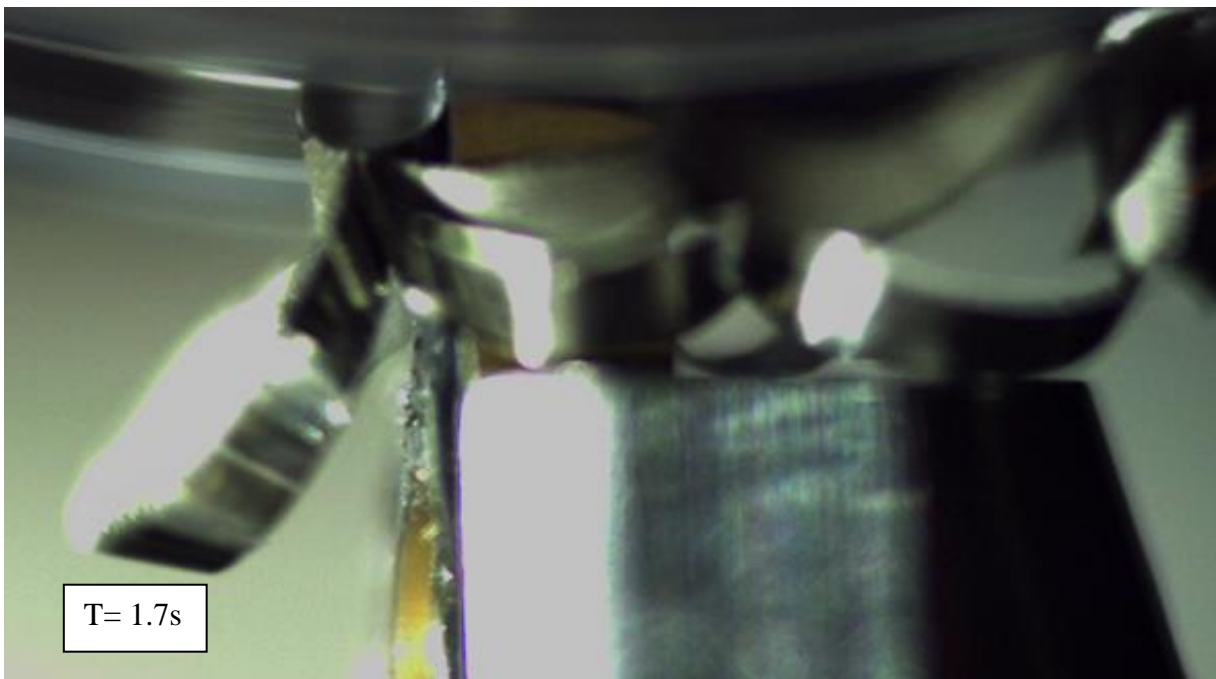
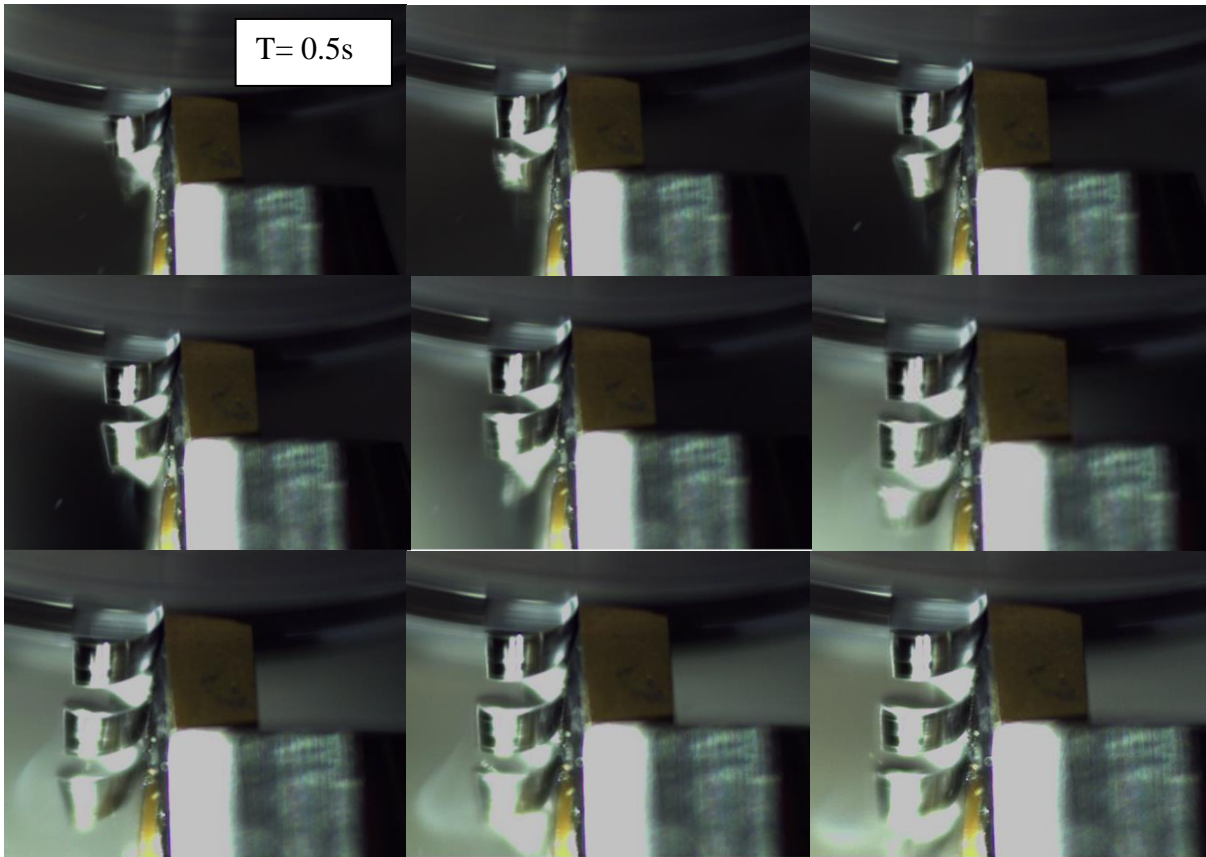


Figure 32: Chip formation without vibration

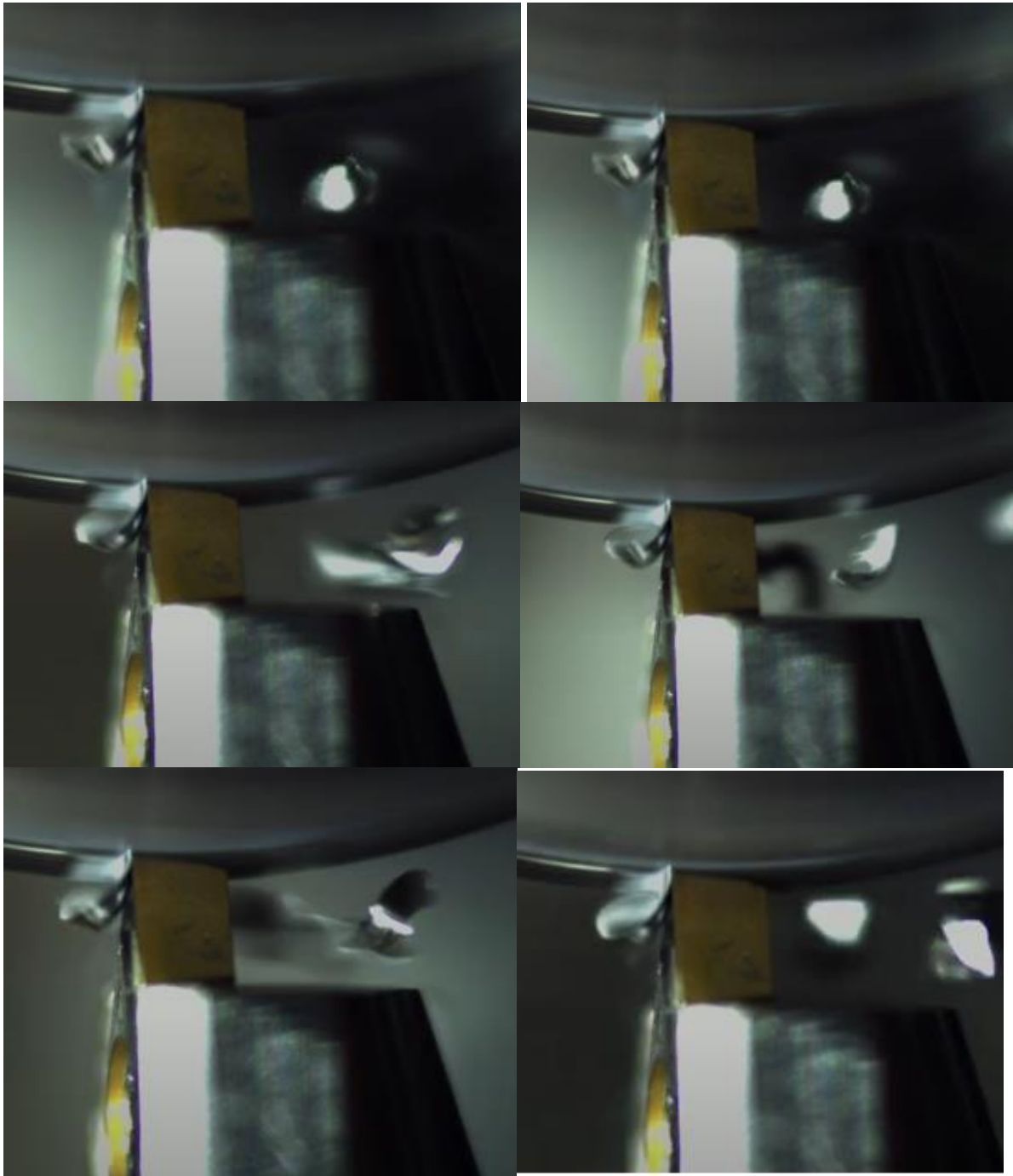


Figure 33: Chip formation with vibration assisted

5. Conclusion

One dimensional radial vibration assisted machining offers distinct advantages over conventional machining (NVAM) related to a finishing operation on a lathe. The surface quality is improved while the cutting parameters are carefully implemented. From the design of experiment, A2B2C3 (Vibration = on; KPAR = 68°; $f = 1.4 \text{ mm/tr}$) is the most appropriate cutting parameters combination to obtain an optimal surface quality $R_a = 1.491 \text{ }\mu\text{m}$ (2D roughness). Adding vibration is the most significant effect on the surface quality providing lower R_a values than NVAM. The cutting forces acquire with the Kistler dynamometer are equivalent in both process (VAM and NVAM).

VAM has demonstrated that applying vibration as a significative influence on the chip removal mechanism. Indeed, the chip fragmentation is facilitated by the VAM process forming arc chip loose which improve surface quality and tool wear resistance by limiting friction due to poor evacuation of the chip. During continuous cutting regime, VAM also helps the insert chips broken to works properly which directly improve de surface roughness. A chip fragmented and ejected directly in the chip tray direction is adequate for tool life and keep a clean surface integrity. An adequate feed should also be defined to contribute to the chip breaker efficiency.

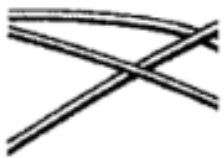












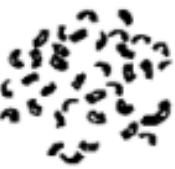




VAM is an efficient technology to obtain specific texture. By combining vertical vibration and feed rate, the texture pattern evolved. The surface shape is mainly influenced by the vibration and the feed parameters. From VAM to NVAM, two different patterns are easily detected (linear and mesh shape), the level intensity depends on the feed rate and the KPAR angle. The surface texture directly influences the ability of the material to resist friction depending on the amount of pick or valley.

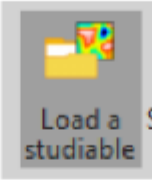
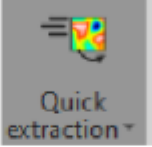

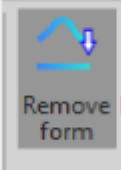
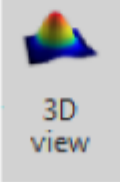
6. Bibliography

- [1] ZhichaoYang, Lida Zhu, Bin Lin, (2020), “Review of ultrasonic vibration-assisted machining in advanced materials”
- [2] Lu Zheng, Wanqun Chen, Dehong Huo, (2020), “Review of vibration devices for vibration-assisted machining”
- [3] Wei-Xing Xu¹, Liang-Chi Zhang, (2015), “Ultrasonic vibration-assisted machining: principle, design and application”
- [4] Astashev V K, Khusnutdinova K, Babitsky ,(2007), “Ultrasonic processes and machines dynamics, control and applications”
- [5] Wanqun Chen, Lu Zheng, Xiangyu Teng, (2018), “Cutting Mechanism Investigation in Vibration-Assisted Machining “
- [6] S. J. Zhang, S. To, S. J. Wang, and Z. W. Zhu, (2015) “A review of surface roughness generation in ultra-precision machining,” International Journal of Machine Tools and Manufacture”
- [7] Ping Zou , Ye He, Hao Wu, (2015), “Experimental Investigation of Ultrasonic Vibration Assisted Turning of 304 Austenitic Stainless Steel”
- [8] GAO, Yuan; SUN, Ronglei; LEOPOLD, Jürgen, (2015) “Analysis of Cutting Stability in Vibration Assisted Machining Using Ananalytical Predictive Force Model”
- [9] Xianfu Liu, Debao Wu, Ping Cui, (2019), “Analysis of surface texturing in radial ultrasonic vibration-assisted turning”
- [10] Sandvik Coromant UK – “How to choose correct turning insert”
- [11] DCMT070204-UF-YG3030 Carbide Turning Inserts (Finishing Chipbreaker) YG-1 - Cutwell
- [12] American Society of Mechanical Engineers, (1996), “Surface Texture: Surface Roughness, Waviness and Lay”
- [13] Michigan Metrology, (2022), “3D surface roughness and wear measurement, analyse and inspection”
- [14] Chris Felix, (2018), “4 Strategies for Managing Chip Control”
- [15] (2020), [YG-1 Turning] « Des solutions de tournage » – YG1 Inserts de tournage
- [16] yg1usa- “7 New grades to optimize turning”

7. Annex

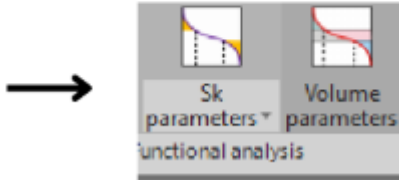
Table G.1 — Chip forms

1 Ribbon chips ¹⁾	2 Tubular chips ¹⁾	3 Spiral chips	4 Washer-type helical chips ¹⁾	5 Conical helical chips ¹⁾	6 Arc chips ²⁾	7 Elemental chips	8 Needle chips
1.1 Long 	2.1 Long 	3.1 Flat 	4.1 Long 	5.1 Long 	6.1 Connected 		
1.2 Short 	2.2 Short 	3.2 Conical 	4.2 Short 	5.2 Short 	6.2 Loose 		
	2.3 Snarled 		4.3 Snarled 	5.3 Snarled 			
1.3 Snarled 							

-  Load a studiable (Type of file :MontainsMap Topography Surface)
-  Quick extraction
Click on quick extraction and select extract area, then you can modify this area according to your needs and goals
-  Axis settings
Click on axis settings and then, select "centred" and "scale". After that, chose the most relevant max and min values.
-  Remove form
Click on "Operators" and then on "Remove form". Finally, click on "OK".
-  3D view
Select your extracted area and in Studies click on "3D view", a 3D view of your sample will appear



Double-click on your 3D view and click on amplification, then select an amplification according to your needs.



Still in the studies' section, you can show the Sk and volume parameters.